Behavioral/Systems/Cognitive

Contribution of Dopamine D1 and D2 Receptors to Amygdala Activity in Human

Hidehiko Takahashi,[1,2] Harumasa Takano,[1] Fumitoshi Kodaka,[1] Ryosuke Arakawa,[1] Makiko Yamada,[1] Tatsui Otsuka,[1] Yoshiyuki Hirano,[2] Hideyuki Kikyo,[1] Yoshiro Okubo,[4] Motoichiro Kato,[5] Takayuki Obata,[2] Hiroshi Ito,[1] and Tetsuya Suhara[1]

Departments of [1]Molecular Neuroimaging and [2]Biophysics, Molecular Imaging Center, National Institute of Radiological Sciences, Chiba 263-8555 Japan, [3]Precursory Research for Embryonic Science and Technology, Japan Science and Technology Agency, Saitama, 332-0012, Japan, [4]Department of Neuropsychiatry, Nippon Medical School, Tokyo 113-8603, Japan, and [5]Department of Neuropsychiatry, Keio University School of Medicine, Tokyo 160-8582, Japan

Several animal studies have demonstrated functional roles of dopamine (DA) D1 and D2 receptors in amygdala activity. However, the contribution of DA D1 and D2 receptors to amygdala response induced by affective stimuli in human is unknown. To investigate the contribution of DA receptor subtypes to amygdala reactivity in human, we conducted a multimodal *in vivo* neuroimaging study in which DA D1 and D2 receptor bindings in the amygdala were measured with positron emission tomography (PET), and amygdala response induced by fearful faces was assessed by functional magnetic resonance imaging (fMRI) in healthy volunteers. We used multimodality voxelwise correlation analysis between fMRI signal and DA receptor binding measured by PET. DA D1 binding in the amygdala was positively correlated with amygdala signal change in response to fearful faces, but DA D2 binding in the amygdala was not related to amygdala signal change. DA D1 receptors might play a major role in enhancing amygdala response when sensory inputs are affective.

Introduction

The amygdala plays a central role in processing affective stimuli, and in particular, threatening stimuli in the brain (LeDoux, 2000). The amygdala receives a moderate innervation of dopaminergic fibers (Asan, 1998), and both dopamine (DA) D1 and D2 receptors are expressed in this region (Ito et al., 2008), although the latter exhibit lower expression (Scibilia et al., 1992). DA release in the amygdala is increased in response to stress (Inglis and Moghaddam, 1999). It has been shown in animal studies that DA potentiates the response of the amygdala by augmenting excitatory sensory input and attenuating inhibitory prefrontal input to the amygdala (Rosenkranz and Grace, 2002). Systemic and local applications into the amygdala of D1 agonist and antagonist are known to potentiate and decrease fear response in animals, respectively. Although some studies reported that applications of D2 agonist and antagonist induced similar effects, the results were less consistent compared with D1-mediated effects (for review, see Pezze and Feldon, 2004; de la Mora et al., 2009).

A human functional magnetic resonance imaging (fMRI) study reported that doparminergic drug therapy such as levodopa or DA agonists partially restored amygdala response due to emotional task in Parkinson's disease patients who showed no significant amygdala response during drug-off states (Tessitore et al., 2002). In addition, another fMRI study of healthy volunteers has demonstrated that amphetamine potentiated the response of the amygdala during an emotional task (Hariri et al., 2002). More recently, Kienast et al. (2008) reported that dopamine storage capacity in human amygdala, measured with 6-[^{18}F]fluoro-L-DOPA positron emission tomography (PET), was positively correlated with functional magnetic resonance imaging (fMRI) signal changes in amygdala. However, the contribution of DA D1 and D2 receptors to amygdala response induced by affective stimuli is unknown in human. To investigate the relation between amygdala reactivity and dopamine receptor subtype, we conducted a multimodal *in vivo* neuroimaging study in which DA D1 and D2 receptor bindings in the amygdala were measured with PET, and amygdala response by novel faces with either neutral or fearful expression was assessed with fMRI. Based on animal pharmacological studies, we hypothesized that D1, but not D2 receptors, would predict amygdala response.

Received Nov. 17, 2009; revised Jan. 8, 2010; accepted Jan. 8, 2010.

This study was supported by a consignment expense for Molecular Imaging Program on "Research Base for PET Diagnosis" from the Ministry of Education, Culture, Sports, Science and Technology. Fukanori Kochiyama and Yoko Ikoma are greatly acknowledged for her comments. We thank K. Tanimoto and I. Shiraishi for their assistance in performing the PET experiments at the National Institute of Radiological Sciences. We also thank Y. Fukushima, K. Suzuki, and I. Izumida of the National Institute of Radiological Sciences for their help as clinical research coordinators.

Correspondence should be addressed to Hidehiko Takahashi, Department of Molecular Neuroimaging, National Institute of Radiological Sciences, 9-1, 4-chome, Anagawa, Inage-ku, Chiba, Chiba 263-8555, Japan. E-mail: hidehiko@nirs.go.jp.

DOI:10.1523/JNEUROSCI.5689-09.2010

 0270-6474/10/303043-05$15.00/0

Materials and Methods

Subjects

Twenty-one male volunteers [mean age 23.1 ± (SD) 3.6 years] were studied. They did not meet the criteria for any psychiatric disorder based on unstructured psychiatric screening interviews. None of the controls were taking alcohol at the time, nor did they have a history of psychiatric disorder, significant physical illness, head injury, neurological disorder, or alcohol or drug dependence. All subjects were right-handed according to the Edinburgh Handedness Inventory. All subjects underwent MRI to rule out cerebral anatomic abnormalities. After complete explanation of the study,

written informed consent was obtained from all subjects, and the study was approved by the Ethics and Radiation Safety Committee of the National Institute of Radiological Sciences, Chiba, Japan.

fMRI procedure

Stimulus materials were taken from the Karolinska Directed Emotional Faces (KDEF) (Lundqvist et al., 1998). Thirty neutral and 30 fear faces were used, with half of them being male faces. The pictures were projected via a computer and a telephoto lens onto a screen mounted on a head-coil. The experimental design consisted of 5 blocks for each of the 2 conditions (neutral, fear) interleaved with 21 s rest periods. The order of presentation for the 2 conditions (neutral and fear) was randomized. During the baseline condition, subjects viewed a crosshair pattern projected to the center of the screen. In each 21 s block, 6 different faces of the same emotional class were presented for 3.5 s each. During the scans, the subjects were instructed to judge the gender of each face using selection buttons.

fMRI scanning

The images were acquired with a 3.0 Tesla Excite system (General Electric). Functional images of 126 volumes were acquired with T2*-weighted gradient echo planar imaging sequences sensitive to the blood oxygenation level-dependent (BOLD) contrast. Each volume consisted of 40 transaxial contiguous slices with a slice thickness of 3 mm to cover almost the whole brain (flip angle, 90°; echo time, 50 ms; repetition time, 3500 ms; matrix, 64 × 64; field of view, 24 × 24 cm).

Analysis of fMRI data

Data analysis was performed with the statistical parametric mapping software package (SPM2) (Wellcome Department of Cognitive Neurology, London, UK) running with MATLAB (MathWorks). All volumes were realigned to the first volume of each session to correct for subject motion and were spatially normalized to the standard space defined by the Montreal Neurological Institute (MNI) template. After normalization, all scans had a resolution of $2 \times 2 \times 2\ mm^3$. Functional images were spatially smoothed with a three-dimensional isotropic Gaussian kernel (full-width at half-maximum of 8 mm). Low-frequency noise was removed by applying a high-pass filter (cutoff period = 128 s) to the fMRI time series at each voxel. A temporal smoothing function was applied to the fMRI time series to enhance the temporal signal-to-noise ratio. Significant hemodynamic changes for each condition were examined using the general linear model with boxcar functions convolved with a hemodynamic response function. Statistical parametric maps for each contrast of *t*-statistic were calculated on a voxel-by-voxel basis.

We assessed the contrasts of fear and neutral minus baseline (F&N-B). A random effects model, which estimates the error variance for each condition across the subjects, was implemented for group analysis. The contrast images were obtained from single-subject analysis and entered into the group analysis. A one-sample *t* test was applied to determine group response for each effect. Significant amygdala activations were identified if they reached the extent threshold of $p < 0.05$ corrected for multiple comparisons, with a height threshold of $p < 0.001$, uncorrected.

PET scanning

After the fMRI session, each participant underwent PET scanning. The interval between fMRI session and PET scan was 3–5 h. PET studies were performed on ECAT EXACT HR+ (CTI-Siemens). The system provides 63 planes and a 15.5 cm field of view. To minimize head movement, a head fixation device (Fixster) was used. A transmission scan for attenuation correction was performed using a germanium 68–gallium 68 source. Acquisitions were done in three-dimensional mode with the interplane septa retracted. For evaluation of D1 receptors, a bolus of 219.7 ± 6.9 MBq of [^{11}C]SCH23390 with specific radioactivities (95.7 ± 35.5 GBq/μmol) was injected intravenously from the antecubital vein with a 20 ml saline flush. For evaluation of extrastriatal DA D2 receptors, a bolus of 218.1 ± 14.7 MBq of [^{11}C]FLB457 with high specific radioactivities (221.6 ± 94.9 GBq/μmol) was injected in the same way. Dynamic half-maximum, 7.5 mm). MRI was performed on Gyroscan NT (Philips Medical Systems) (1.5 T). T1-weighted images of the brain were obtained for all subjects. Scan parameters were 1-mm-thick, three-dimensional T1 images with a transverse plane (repetition time/echo time, 19/10 ms; flip angle, 30°; scan matrix, 256 × 256 pixels; field of view, 256 × 256 mm; and number of excitations, 1).

Quantification of DA D1 and D2 receptors

Quantitative analysis was performed using the three-parameter simplified reference tissue model (Lammertsma and Hume, 1996; Olsson et al., 1999). The cerebellum was used as a reference region because it has been shown to be almost devoid of DA D1 and D2 receptors (Farde et al., 1987; Olsson et al., 1999; Suhara et al., 1999). The model provides an estimation of the binding potential ($BP_{ND\ (nondisplaceable)}$) (Innis et al., 2007), which is defined by the following equation: $BP_{ND} = k_3/k_4 = f_2 B_{max}/K_d\ [1 + \Sigma_i F_i/K_{di}]$, where k_3 and k_4 describe the bidirectional exchange of tracer between the free compartment and the compartment representing specific binding, f_2 is the "free fraction" of nonspecifically bound radioligand in brain, B_{max} is the receptor density, K_d is the equilibrium dissociation constant for the radioligand, and F_i and K_{di} are the free concentration and dissociation constant of competing ligands, respectively (Lammertsma and Hume, 1996). Tissue concentrations of the radioactivities of [^{11}C]SCH23390 and [^{11}C]FLB457 were obtained from regions of interest (ROIs) defined on PET images of summated activity for 60 min and 90 min, respectively, with reference to the individual MRIs coregistered on summated PET images and the brain atlas. Given our hypothesis of amygdala activation during viewing novel neutral and fearful faces, ROIs were set on the bilateral amygdala. The method for defining the boundaries of the amygdala was adapted from previously described methods (Kates et al., 1997; Convit et al., 1999). In short, the amygdala ROIs consisted of three axial slices. The anterior and posterior boundaries were identified at the level of the optic chiasm and the temporal horn of the lateral ventricle, respectively. The superior and inferior-lateral boundaries were identified at the level of the mammalian body and the temporal lobe white matter and extension of the temporal horn, respectively. We also created parametric images of BP_{ND} using the basis function method (Gunn et al., 1997) to conduct voxelwise SPM analysis in addition to ROI analysis.

Statistical analysis

ROI correlation analysis. Estimates of percentage signal change of fear vs baseline condition were extracted from the amygdala for each participant using the MarsBaR toolbox (Brett et al., 2002). The bilateral amygdala ROIs were defined from the WFU-Pickatlas SPM tool (Maldjian et al., 2003) with the aal atlas (Tzourio-Mazoyer et al., 2002). Correlation between BP_{ND} of [^{11}C]SCH23390 and [^{11}C]FLB457 in the bilateral amygdala and bilateral amygdala fMRI signal change were calculated using SPSS.

Confirmatory SPM correlation analysis. Parametric images of BP_{ND} of [^{11}C]SCH23390 and [^{11}C]FLB457 were analyzed using SPM2. Exactly the same image preprocessings of normalization and smoothing that were used in fMRI data analysis were applied to parametric images of BP_{ND}. To conduct multimodality voxelwise correlation analysis between the BOLD signal and DA receptor binding, we used the biological parametric mapping toolbox for SPM (Casanova et al., 2007). Significant clusters were identified if they reached the extent threshold of $p < 0.05$ corrected for multiple comparisons, with a height threshold of $R > 0.6$ ($p < 0.003$ uncorrected).

Results

Since the face pictures consisted of Caucasian faces (racial outgroup), even novel neutral faces produced amygdala response in several participants (Hart et al., 2000; Schwartz et al., 2003), leading to a blunted contrast of fear minus neutral. Therefore, we combined neutral and fear conditions and used F&N-B contrast

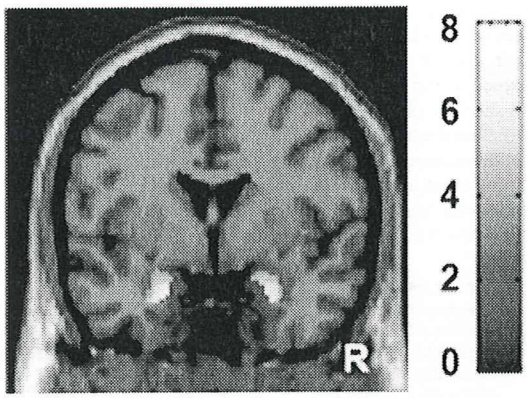

Figure 1. Images showing brain response induced by fear and neutral minus baseline condition. Bilateral amygdala responses are shown. The bar shows the range of the *t*-value. R indicates right.

voxels] (Fig. 1). The mean BP_{ND} of [^{11}C]SCH23390 in the right and left amygdala were 0.38 ± 0.08 and 0.39 ± 0.11, respectively. The mean BP_{ND} of [^{11}C]FLB457 in the right and left amygdala were 2.49 ± 0.50 and 2.50 ± 0.44, respectively.

Correlation analysis of biological parametric mapping revealed that the BP_{ND} value of [^{11}C]SCH23390 in the right amygdala was positively correlated with the BOLD signals in the right amygdala of F&N-B contrast [peak (28, 2, −28), 24 voxels] (Fig. 2A). ROIs analysis also revealed a similar significant correlation ($r = 0.59$, $p = 0.005$) in the right amygdala (Fig. 2B), but not in the left amygdala ($r = 0.18$, $p = 0.43$). According to biological parametric mapping analysis, the BP_{ND} value of [^{11}C]FLB457 in the amygdala was not correlated with BOLD signals in the amygdala of F&N-B contrast. ROIs analysis showed that right and left amygdala D2 binding was not correlated with the BOLD signals in the right ($r = 0.26$, $p = 0.27$) and left amygdala ($r = 0.28$, $p = 0.23$), respectively. Both biological parametric mapping analysis and ROIs analysis showed that D1 binding in the right and left amygdala was not correlated with D2 binding in the right ($r = 0.24$, $p = 0.30$) and left amygdala ($r = 0.16$, $p = 0.49$), respectively. We used anatomically defined ROIs of the amygdala rather than functional ROIs defined by fMRI in the ROI correlation analysis because it is difficult to place functionally defined ROIs on individual PET data. Anatomically defined ROIs of the amygdala were larger than functionally defined amygdala ROIs. This fact was advantageous in increasing the signal-to-noise ratio in the PET analysis, but led to blunted BOLD signal changes in the amygdala. However, BOLD signal changes derived from both ROI methods were highly correlated with each other. For example, very high correlation ($r = 0.80$, $p < 0.001$) was observed in the right amygdala. Thus, regardless of ROI definition method, we obtained similar results from ROI correlation analyses between BOLD signal changes and DA receptor binding in the amygdala.

Discussion

Using a multimodality *in vivo* neuroimaging approach, we first directly compared amygdala DA D1 and D2 receptor bindings, indices of receptor availability, with amygdala response evoked by novel or fearful stimuli in human. We found that DA D1 receptors, but not D2 receptors, predicted amygdala response induced by novel facial stimuli with either neutral or fearful expression. Our findings broaden our knowledge about dopaminergic transmission in amygdala response beyond the recent study (Kienast et al., 2008) that elucidated the relation between presynaptic dopamine synthesis and amygdala reactivity.

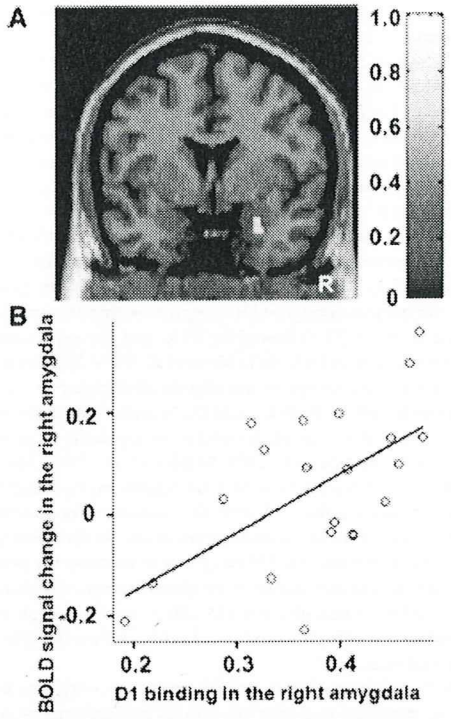

Figure 2. ***A***, SPM correlation analysis revealed significant positive linear correlations between D1 binding in the right amygdala and right amygdala signal change. The bar shows the range of the correlation coefficient. ***B***, ROI correlation analysis also revealed similar correlations. R indicates right.

Human neuroimaging studies reported that DA potentiated amygdala response evoked by affective stimuli (Hariri et al., 2002; Tessitore et al., 2002). In rat studies, Rosenkranz and Grace (2002) demonstrated that DA enhances the response of the amygdala by augmenting excitatory sensory input via DA D2 receptor stimulation and attenuating inhibitory prefrontal input to the amygdala through DA D1 receptor stimulation. More recently, it was demonstrated that both D1 and D2 receptor stimulations directly enhanced the excitability of amygdala projection neurons via postsynaptic mechanism (Rosenkranz and Grace, 2002; Kröner et al., 2005; Yamamoto et al., 2007). Amygdala projection neurons are under inhibitory control by GABAergic interneurons (Royer et al., 1999). Both projection neurons and interneurons in the amygdala express DA D1 and D2 receptors (Rosenkranz and Grace, 1999). It has been shown that DA and D1 receptor stimulation augments interneuron excitability and increases the frequency of IPSC in amygdala projection neurons (Kröner et al., 2005). This is a counterintuitive result, considering the fact that DA disinhibits amygdala response *in vivo*. However, Marowsky et al. (2005) found that a subpopulation of amygdala interneurons (paracapsular intercalated cells), located between the major input and output stations of amygdala, is suppressed by DA through D1 receptor stimulation. DA D2 receptors also play a role in disinhibiting amygdala response by decreasing inhibi-

tion onto projection neurons and increasing inhibition onto interneurons (Bissière et al., 2003).

Although detailed examination of subnuclei of the amygdala is difficult in this imaging method, the dorsal portion of the amygdala roughly corresponds to the central nuclei of amygdala (CeA) and the ventral portion of the amygdala corresponds to the basolateral nuclei of amygdala (BLA) and intercalated cell masses (ICM) (Whalen et al., 2009). The amygdala clusters identified both in fMRI task effect analysis and in correlation analysis between D1 binding and amygdala reactivity were located in the ventral portion of the amygdala. Thus, our findings seem to mainly reflect BLA and ICM properties. It is worth mentioning that the highest density of D1 receptors within the amygdala was found in the ICM, followed by BLA, and the expression of D1 receptors is low in CeA (de la Mora et al., 2009; Muly et al., 2009). In contrast, D2 receptors are mainly distributed in CeA (de la Mora et al., 2009). Both D1 and D2 receptors are expressed both postsynaptically in dendrites and presynaptically in axon terminals (Pinto and Sesack, 2008; Muller et al., 2009; Muly et al., 2009), but D1 receptors in BLA are mainly expressed in the dendrites, indicating that DA directly modulates the excitability of BLA projection neurons and interneurons. At the same time, DA also acts on presynaptic D1 receptors to increase the probability of neurotransmitter release from glutamatergic terminals (Muly et al., 2009). Thus, the net DA effect on D1 receptors in the amygdala is a complex mixture of post- and presynaptic actions at several sites.

Although both DA D1 and D2 receptors contribute to potentiating amygdala response via various mechanisms as described above, our finding suggested that DA D1 receptors play a major role in the overall potentiation of amygdala response. At a behavioral level, previous animal studies repeatedly reported that D1 agonist and antagonist applications into the amygdala potentiated and decreased fear response, respectively. However, the effects of D2 agonist/antagonist on fear response have not been well established (Pezze and Feldon, 2004; de la Mora et al., 2009). Thus, the current finding could be regarded as being consistent with previous behavioral pharmacological studies. The combination of PET molecular imaging and fMRI seems to represent a powerful approach for understanding molecular functions in system neuroscience. However, this study has several limitations. First, current PET techniques for human do not have enough spatial resolution to distinguish subnuclei of the amygdala. Although analysis of parametric images of BP_{ND} has become well established (Gunn et al., 1997) and is used in many [^{11}C]SCH23390 and [^{11}C]FLB457 studies (Cervenka et al., 2006; Takahashi et al., 2008; Karlsson et al., 2009; McNab et al., 2009), a very small region or a single voxel is susceptible to partial volume effect. Thus, it is recommended that parametric image analysis should be used in combination with ROI analysis. At the same time, current results merit further investigation with a higher resolution PET scanner. Second, PET imaging cannot tell us the exact location of DA receptors expressed in projection neurons and interneurons. Future animal studies or *in vitro* studies would complement our findings to determine which D1 receptor-mediated mechanism is most responsible for the overall amygdala response. Third, differences in DA receptor occupancies by endogenous DA might affect BP, leading to different excitabilities of neurons. It is known that BP of [11C]SCH23390 is not sensitive to competitive endogenous dopamine even if massive dopamine is released by amphetamine (Abi-Dargham et al., 1999; Chou et al., 1999). However, it is possible that differences in receptor affinity might contribute to differences in DA receptor occupancies, although Farde et al. (1995) reported that variability in D2 receptor affinity is smaller than that in D2 receptor density. Finally, gender and race effects might also be possible. Any generalization should be approached with caution. Notwithstanding these limitations, we expect our finding to contribute to a broadening of the knowledge of the molecular mechanism of functional abnormalities of the amygdala implicated in neuropsychiatric disorders such as schizophrenia (Takahashi et al., 2004), depression (Drevets, 2000) and Parkinson's disease (Tessitore et al., 2002).

References

Abi-Dargham A, Simpson N, Kegeles L, Parsey R, Hwang DR, Anjilvel S, Zea-Ponce Y, Lombardo I, Van Heertum R, Mann JJ, Foged C, Halldin C, Laruelle M (1999) PET studies of binding competition between endogenous dopamine and the D1 radiotracer [^{11}C] NNC 756. Synapse 32:93–109.

Asan E (1998) The catecholaminergic innervation of the rat amygdala. Adv Anat Embryol Cell Biol 142:1–118.

Bissière S, Humeau Y, Lüthi A (2003) Dopamine gates LTP induction in lateral amygdala by suppressing feedforward inhibition. Nat Neurosci 6:587–592.

Brett M, Anton J, Valabregue R, Poline J (2002) Region of interest analysis using the Marsbar toolbox [abstract]. Paper presented at 8th International Conference on Functional Mapping of the Human Brain, Sendai, Japan.

Casanova R, Srikanth R, Baer A, Laurienti PJ, Burdette JH, Hayasaka S, Flowers L, Wood F, Maldjian JA (2007) Biological parametric mapping: a statistical toolbox for multimodality brain image analysis. Neuroimage 34:137–143.

Cervenka S, Pålhagen SE, Comley RA, Panagiotidis G, Gyselenyi Z, Matthews JC, Lai RY, Halldin C, Farde L (2006) Support for dopaminergic hypoactivity in restless legs syndrome: a PET study on D2-receptor binding. Brain 129:2017–2028.

Chou YH, Karlsson P, Halldin C, Olsson H, Farde L (1999) A PET study of D1-like dopamine receptor ligand binding. Psychopharmacology 146:220–227.

Convit A, McHugh P, Wolf OT, de Leon MJ, Bobinski M, De Santi S, Roche A, Tsui W (1999) MRI volume of the amygdala: a reliable method allowing separation from the hippocampal formation. Psychiatry Res 90:113–123.

de la Mora MP, Gallegos-Cari A, Arizmendi-Garcia Y, Marcellino D, Fuxe K (2009) Role of dopamine receptor mechanisms in the amygdaloid modulation of fear and anxiety: structural and functional analysis. Prog Neurobiol. Advance online publication. Retrieved October 21, 2009. doi:10.1016/j.pneurobio.2009.10.010.

Drevets WC (2000) Functional anatomical abnormalities in limbic and prefrontal cortical structures in major depression. Prog Brain Res 126:413–431.

Farde L, Halldin C, Stone-Elander S, Sedvall G (1987) PET analysis of human dopamine receptor subtypes using 11C-SCH 23390 and 11C-raclopride. Psychopharmacology (Berl) 92:278–284.

Farde L, Hall H, Pauli S, Halldin C (1995) Variability in D2-dopamine receptor density and affinity: a PET study with [^{11}C] raclopride in man. Synapse 20:200–208.

Gunn RN, Lammertsma AA, Hume SP, Cunningham VJ (1997) Parametric imaging of ligand-receptor binding in PET using a simplified reference region model. Neuroimage 6:279–287.

Hariri AR, Mattay VS, Tessitore A, Fera F, Smith WG, Weinberger DR (2002) Dextroamphetamine modulates the response of the human amygdala. Neuropsychopharmacology 27:1036–1040.

Hart AJ, Whalen PJ, Shin LM, McInerney SC, Fischer H, Rauch SL (2000) Differential response in the human amygdala to racial outgroup vs ingroup face stimuli. Neuroreport 11:2351–2355.

Inglis FM, Moghaddam B (1999) Dopaminergic innervation of the amygdala is highly responsive to stress. J Neurochem 72:1088–1094.

Innis RB, Cunningham VJ, Delforge J, Fujita M, Gjedde A, Gunn RN, Holden J, Houle S, Huang SC, Ichise M, Iida H, Ito H, Kimura Y, Koeppe RA, Knudsen GM, Knuuti J, Lammertsma AA, Laruelle M, Logan J, Maguire RP, et al. (2007) Consensus nomenclature for in vivo imaging of reversibly binding radioligands. J Cereb Blood Flow Metab 27:1533–1539.

Ito H, Takahashi H, Arakawa R, Takano H, Suhara T (2008) Normal data-

base of dopaminergic neurotransmission system in human brain measured by positron emission tomography. Neuroimage 39:555–565.
Karlsson S, Nyberg L, Karlsson P, Fischer H, Thilers P, Macdonald S, Brehmer Y, Rieckmann A, Halldin C, Farde L, Bäckman L (2009) Modulation of striatal dopamine D1 binding by cognitive processing. Neuroimage 48:398–404.
Kates W, Abrams M, Kaufmann W, Breiter S, Reiss A (1997) Reliability and validity of MRI measurement of the amygdala and hippocampus in children with fragile X syndrome. Psychiatry Res 75:31–48.
Kienast T, Hariri AR, Schlagenhauf F, Wrase J, Sterzer P, Buchholz HG, Smolka MN, Gründer G, Cumming P, Kumakura Y, Bartenstein P, Dolan RJ, Heinz A (2008) Dopamine in amygdala gates limbic processing of aversive stimuli in humans. Nat Neurosci 11:1381–1382.
Kröner S, Rosenkranz JA, Grace AA, Barrionuevo G (2005) Dopamine modulates excitability of basolateral amygdala neurons in vitro. J Neurophysiol 93:1598–1610.
Lammertsma AA, Hume SP (1996) Simplified reference tissue model for PET receptor studies. Neuroimage 4:153–158.
LeDoux JE (2000) Emotion circuits in the brain. Annu Rev Neurosci 23:155–184.
Lundqvist D, Flykt A, Ohman A (1998) The Karolinska Directed Emotional Faces. Psychology section, Department of Clinical Neuroscience, Karolinska Institute, Stockholm, Sweden.
Maldjian JA, Laurienti PJ, Kraft RA, Burdette JH (2003) An automated method for neuroanatomic and cytoarchitectonic atlas-based interrogation of fMRI data sets. Neuroimage 19:1233–1239.
Marowsky A, Yanagawa Y, Obata K, Vogt KE (2005) A specialized subclass of interneurons mediates dopaminergic facilitation of amygdala function. Neuron 48:1025–1037.
McNab F, Varrone A, Farde L, Jucaite A, Bystritsky P, Forssberg H, Klingberg T (2009) Changes in cortical dopamine D1 receptor binding associated with cognitive training. Science 323:800–802.
Muller JF, Mascagni F, McDonald AJ (2009) Dopaminergic innervation of pyramidal cells in the rat basolateral amygdala. Brain Struct Funct 213:275–288.
Muly EC, Senyuz M, Khan ZU, Guo JD, Hazra R, Rainnie DG (2009) Distribution of D1 and D5 dopamine receptors in the primate and rat basolateral amygdala. Brain Struct Funct 213:375–393.
Olsson H, Halldin C, Swahn CG, Farde L (1999) Quantification of [11C]FLB 457 binding to extrastriatal dopamine receptors in the human brain. J Cereb Blood Flow Metab 19:1164–1173.
Pezze MA, Feldon J (2004) Mesolimbic dopaminergic pathways in fear conditioning. Prog Neurobiol 74:301–320.
Pinto A, Sesack SR (2008) Ultrastructural analysis of prefrontal cortical inputs to the rat amygdala: spatial relationships to presumed dopamine axons and D1 and D2 receptors. Brain Struct Funct 213:159–175.
Rosenkranz JA, Grace AA (1999) Modulation of basolateral amygdala neuronal firing and afferent drive by dopamine receptor activation in vivo. J Neurosci 19:11027–11039.
Rosenkranz JA, Grace AA (2002) Cellular mechanisms of infralimbic and prelimbic prefrontal cortical inhibition and dopaminergic modulation of basolateral amygdala neurons *in vivo*. J Neurosci 22:324–337.
Royer S, Martina M, Paré D (1999) An inhibitory interface gates impulse traffic between the input and output stations of the amygdala. J Neurosci 19:10575–10583.
Schwartz CE, Wright CI, Shin LM, Kagan J, Whalen PJ, McMullin KG, Rauch SL (2003) Differential amygdalar response to novel versus newly familiar neutral faces: a functional MRI probe developed for studying inhibited temperament. Biol Psychiatry 53:854–862.
Scibilia RJ, Lachowicz JE, Kilts CD (1992) Topographic nonoverlapping distribution of D1 and D2 dopamine receptors in the amygdaloid nuclear complex of the rat brain. Synapse 11:146–154.
Suhara T, Sudo Y, Okauchi T, Maeda J, Kawabe K, Suzuki K, Okubo Y, Nakashima Y, Ito H, Tanada S, Halldin C, Farde L (1999) Extrastriatal dopamine D2 receptor density and affinity in the human brain measured by 3D PET. Int J Neuropsychopharmacol 2:73–82.
Takahashi H, Koeda M, Oda K, Matsuda T, Matsushima E, Matsuura M, Asai K, Okubo Y (2004) An fMRI study of differential neural response to affective pictures in schizophrenia. Neuroimage 22:1247–1254.
Takahashi H, Kato M, Takano H, Arakawa R, Okumura M, Otsuka T, Kodaka F, Hayashi M, Okubo Y, Ito H, Suhara T (2008) Differential contributions of prefrontal and hippocampal dopamine D1 and D2 receptors in human cognitive functions. J Neurosci 28:12032–12038.
Tessitore A, Hariri AR, Fera F, Smith WG, Chase TN, Hyde TM, Weinberger DR, Mattay VS (2002) Dopamine modulates the response of the human amygdala: a study in Parkinson's disease. J Neurosci 22:9099–9103.
Tzourio-Mazoyer N, Landeau B, Papathanassiou D, Crivello F, Etard O, Delcroix N, Mazoyer B, Joliot M (2002) Automated anatomical labeling of activations in SPM using a macroscopic anatomical parcellation of the MNI MRI single-subject brain. Neuroimage 15:273–289.
Whalen PJ, Davis C, Oler JA, Kim H, Kim J, Neta M (2009) Human amygdala responses to facial expressions of emotions. In: The human amygdala (Whalen PJ, Phelps EA, eds), pp 265–288. New York: Guilford.
Yamamoto R, Ueta Y, Kato N (2007) Dopamine induces a slow afterdepolarization in lateral amygdala neurons. J Neurophysiol 98:984–992.

Neuroscience Research 63 (2009) 115–121

Contents lists available at ScienceDirect

Neuroscience Research

journal homepage: www.elsevier.com/locate/neures

Time estimation during sleep relates to the amount of slow wave sleep in humans

Sayaka Aritake-Okada [a,b,*], Makoto Uchiyama [c], Hiroyuki Suzuki [a], Hirokuni Tagaya [d], Kenichi Kuriyama [e], Masato Matsuura [b], Kiyohisa Takahashi [f], Shigekazu Higuchi [a], Kazuo Mishima [a]

[a] Department of Psychophysiology, National Institute of Mental Health, National Center of Neurology and Psychiatry, Tokyo, Japan
[b] Department of Life Sciences and Bio-informatics, Graduate School of Allied Health Sciences, Tokyo Medical and Dental University, Tokyo, Japan
[c] Department of Neuropsychiatry, Nihon University School of Medicine, Tokyo, Japan
[d] Department of Health Science, School of Allied Health Sciences, Kitasato University, Japan
[e] Department of Adult Mental Health, National Institute of Mental Health, National Center of Neurology and Psychiatry, Tokyo, Japan
[f] Japan Foundation for Neuroscience and Mental Health, Tokyo, Japan

ARTICLE INFO

Article history:
Received 14 July 2008
Received in revised form 14 October 2008
Accepted 6 November 2008
Available online 14 November 2008

Keywords:
Time estimation
Interval timing clock
Cognitive science
Sleep
Circadian phase
Insomnia

ABSTRACT

Humans have the ability to estimate the amount of time that has elapsed during sleep (time estimation ability; TEA) that enables a subset of individuals to wake up at a predetermined time without referring to a watch or alarm clock. Although previous studies have indicated sleep structure as a key factor that might influence TEA during sleep, which sleep parameters could affect the TEA has not been clarified. We carried out an experimental study in which 20 healthy volunteers participated in six time estimation trials during the 9-h nighttime sleep (NS) experiment or daytime sleep (DS) experiment. The time estimation ratio (TER, ratio of the subjective estimated time interval to actual time interval) decreased significantly from the first to the sixth trial in both the NS and DS experiments. TER correlated positively with slow wave sleep (SWS) in both experiments, suggesting that SWS was a determining factor in accurate time estimation, irrespective of circadian phase they slept. No other sleep parameters showed steady influence on TEA. The present findings demonstrate that longer period of SWS is associated with the longer sleep time they subjectively experienced during sleep.

1. Introduction

Growing evidence suggests that humans have the ability to estimate the amount of time that has elapsed on the order of milliseconds to several hours (time estimation ability, TEA) even under circumstances in which external time information is not available (Morell, 1996; Harrington et al., 1998; Lalonde and Hannequin, 1999; Rao et al., 2001; Ivry and Spencer, 2004). A series of studies has supported the notion that the TEA pervades sleep period; humans perceive the amount of time that has passed during sleep (Lewis, 1969; Tart, 1970; Zung and Wilson, 1971; Bell, 1972; Moiseeva, 1975; Lavie et al., 1979; Hartocollis, 1980; Campbell, 1986; Zepelin, 1986; Hawkins, 1989; Moorcroft et al., 1997; Born et al., 1999; Kaida et al., 2003; Aritake et al., 2004; Fichten et al., 2005). This ability enables a subset of individuals to wake up at a predetermined time without referring to a watch or alarm clock. Moorcroft et al. (1997) referred to this phenomenon as "self-awakening", and Born et al. (1999) referred to it as "anticipated sleep termination". Actually, several studies have reported that more than half of individuals surveyed were able to achieve "self-awakening" with a margin of error of plus or minus 10-odd min (Lavie et al., 1979; Moorcroft et al., 1997).

A large part of the physiological mechanism of TEA remains unclear, but previous studies have shown that several physiological and psychological factors influence TEA during sleep. These include psychological status prior to bedtime (Hawkins, 1989) altered neuroendocrine tonus (Born et al., 1999), and sleep structure (Kleitman, 1963; Tart, 1970; Zung and Wilson, 1971; Lavie et al., 1979; Zepelin, 1986; Antake et al., 2004) preceding the predetermined wake time. For instance, strong motivation and the confidence that are will wake up at the predetermined time are associated with successful self-awakening (Hawkins, 1989; Moorcroft et al., 1997). Born et al. (1999) showed clearly that anticipated awakening at a predetermined time was preceded by an elevation in ACTH secretion (a particularly early, morning ACTH surge), a phenomenon that did not occur in relation to an unexpected ("surprise") awakening at the same clock time.

Several studies have focused on sleep structure as a key factor that might influence TEA during sleep; however, it remains controversial whether the preceding sleep stage or partial

* Corresponding author at: Department of Psychophysiology, Institute of Mental Health, National Center of Neurology and Psychiatry, Ogawa-higashicho 4-1-1, Kodaira, Tokyo 187-8502, Japan. Tel.: +81 42 346 2014; fax: +81 42 346 2072.
E-mail address: sayaca@ncnp.go.jp (S. Aritake-Okada).

0168-0102/$ – see front matter © 2008 Elsevier Ireland Ltd and the Japan Neuroscience Society. All rights reserved.
doi:10.1016/j.neures.2008.11.001

awakening prior to the predetermined wake time modifies TEA in humans (Kleitman, 1963; Zung and Wilson, 1971; Lavie et al., 1979; Zepelin, 1986; Aritake et al., 2004). We previously conducted a study to test whether the preceding sleep structure influenced the estimated passage of time during nighttime sleep which was divided into six time periods (90 min each) in healthy young subjects (Aritake et al., 2004). We found that, as sleep progressed, the subjects underestimated the amount of time that had passed in each time period. The estimated elapsed time correlated positively with the amount of slow wave sleep (SWS) and negatively with the amount of REM sleep. These findings support the notion that TEA pervades sleep and that it is affected by the preceding sleep status.

The aim of the present study was to clarify which sleep parameters could essentially influence on TEA by comparing the properties of estimated time interval during the usual nighttime sleep (NS) period with those during an arbitrary daytime sleep (DS) period in circadian antiphase. We expected REM sleep and SWS to show different time distributions between the two experimental conditions, and that this would enable us to more precisely detect functional interaction between the sleep structure and TEA during the sleep period.

2. Materials and methods

2.1. Participants

Twenty healthy men aged 18–23 years (mean, 21.1 ± 1.7 years), who had regular sleep habits, participated in the study. They were randomly allocated to on NS experiment or DS experiment. Three participants allocated to the DS experiment withdrew from the study (one due to infection during the pre-study period, one for an undisclosed reason, and one due to discomfort during the acute shift schedule). Thus, 10 participants completed the NS experiment (mean age, 20.2 ± 1.6 years) and 7 completed the DS experiment (mean age, 22.4 ± 0.7 years). They provided written informed consent after the possible risks and details of the study were explained to them. A physician and a psychiatrist examined all participants and found that none suffered from a neurological or psychiatric disorder, and none had a history of psychoactive drug use. Participants were instructed to keep to a regular sleep–wake schedule; record their sleep patterns in a sleep log; and abstain from caffeine, nicotine, and alcohol for 1 week prior to the experiment. All participants wore a wrist activity recorder (Actiwatch-L, Mini-Mitter Co., Inc., Bend, OR, USA) for 1 week prior to the experiment. Sleep onset and offset times were determined with Actiware Sleep software (V3.2 Mini-Mitter Co., Inc.). The details recorded in participants' sleep logs, together with their sleep onset and offset times, were used to confirm that they had regular sleep–wake schedules. Because participants' attention to time could potentially affect the experimental results, we told them that the aim of the study was to investigate correlation between sleep parameters and subjective feeling; we did not disclose the study objectives until the end of the study. We confirmed that none of the participants had sensed the real purpose of the investigation until the end of this study. The study protocol was approved by the Institutional Review Board of the National Center of Neurology and Psychiatry.

2.2. Experimental procedures

Time estimation protocol is illustrated in Fig. 1.

2.2.1. NS experiment

The NS experiment was begun as follows: on day 1, the participant arrived at the laboratory at 19:00 h and slept in the laboratory bedroom from 0:00 h to 08:00 h for adaptation. After being woken at 08:00 h on day 2, the participant was kept awake until 00:00 h on day 3 under dim light conditions (150 lx). During waking hours, the participant was kept from knowing the clock time until the beginning of the time estimation protocol (TEP). His only awareness of the time of day would have been by the scheduled provision of an isocaloric meal (450 kcal) and mineral water every 4 h. At 00:00 h on day 3, the participant was instructed to go to bed and that the TEP would begin.

2.2.2. DS experiment

The DS experiment was begun as follows: on day 1, the participant arrived at the laboratory at 19:00 h and slept in the laboratory bedroom from 0:00 h to 08:00 h for adaptation. After being woken at 08:00 h on day 2, the participant was kept awake for 28 h until 12:00 h on day 3 under the same isolated condition as in the NS experiment. An isocaloric meal (450 kcal) and mineral water were provided every 4 h. After 28 h of enforced wakefulness,

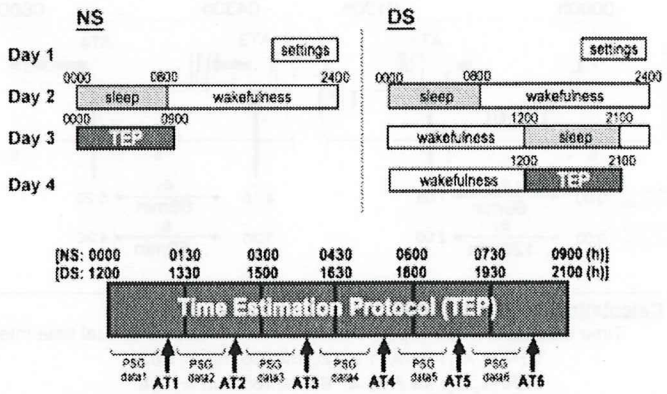

Fig. 1. Time estimation protocol (TEP). TEP was conducted between 00:00 h and 09:00 h (nighttime sleep: NS) or 12:00 h and 21:00 h (daytime sleep: DS). The 9-h polysomnography (PSG) recording periods were divided into six 90-min periods. We woke the participants and conducted a structured interview once during each 90-min period (awakening trial: AT). Participants were awakened for an AT when (1) they had slept for longer than 45 min after lights out or since the end of the prior AT; and (2) stage 2 sleep had continued for more than 3 min. PSG data between successive ATs were obtained. If these criteria were not satisfied until 75 min after the beginning of 90-min period, the participants were awakened at the end of each 90-min period. In the structured interview, we asked the several questions including, "What time do you think it is now? (subjective time of day)" to determine participants' spontaneous estimation of time, without encouraging them to focus their attention on time.

the participant was allowed recovery sleep from 12:00 h to 21:00 h on day 3. After being woken at 21:00 h on day 3, the participant was kept awake for 15 h. At 12:00 h on day 4, the participant was instructed to go to bed and that the TEP would begin.

2.3. Measures and condition

All experiments were performed in the time isolation laboratory of the National Center of Neurology and Psychiatry in Japan. Polysomnography (PSG) comprised electroencephalogram (EEG; C3–A2, C4–A1 and O1–A2, O2–A1) in conformity with the 10–20 electrode system, electrooculogram (EOG; left–A2 and right–A1), chin surface electromyogram (chin–EMG), and electrocardiogram (ECG) recordings. PSG data were obtained continuously during each experiment and stored in a digital EEG system (Neurofax, Nihon Kohden, Tokyo, Japan). Core body temperature (cBT) was measured every 2 min from 21:00 h on day 1 until the end of the experiment, the data were stored in a soft ware (V3.2 Mini-Mitter Co., Inc.). The PSG and cBT monitoring were set up between 19:00 h and 21:00 h on day 1. The participant' behavioral status and sleep–wake status were continuously monitored by two well-trained research attendants using a digital EEG system and by visual observation. Room temperature and humidity were controlled at 24 °C and 60%, respectively.

2.4. Time estimation protocol

The 9-h PSG recording period was divided into six 90-min periods (Fig. 1). During each 90-min period, the participant was awakened and given a brief structured interview with supine (lasting 2 min or less, <8 lx) about the perceived clock time. This procedure was termed the awakening trial (AT). The time of each AT was determined when (1) the participant had slept for more than 45 min after lights-out or since the end of the prior AT; and (2) stage 2 sleep had continued for more than 3 min. If these criteria were not satisfied before 75 min of each 90-min period has passed, the participant was awakened at the end of the 90-min period. During the structured interview, we asked several questions including, "What time do you think it is now?" to determine the participant's spontaneous estimation of time, without encouraging him to focus his attention on the amount of time that had passed since previous arousal. The interviewer was instructed not to give disclose the real purpose of the study, and the participant was given no information on the exact number or timing of the ATs.

2.5. Data analysis

2.5.1. TEA variables

The subjective time interval, defined as the difference between the estimated time of day during the AT and that during the previous AT (or 00:00 h) was determined. Time estimation ratio (TER), defined as the estimated time interval (subjective time interval: s_1 or s_2) divided by the actual clock time interval (actual time interval: a_1 or a_2) (Aritake et al., 2004) (Fig. 2), was also determined.

2.5.2. Sleep parameters

PSG data obtained between successive ATs were scored in epochs of 30 s according to the standard criteria (Rechtschaffen and Kales, 1968). Time percentages of stage W (%stage W), stage 1 (%stage 1), stage 2 (%stage 2), stage 3 + 4 (%stage 3 + 4) and stage REM (%stage REM) sleep for the entire sleep period and for each AT period were calculated for all PSG recordings.

2.5.3. cBT

To ensure comparability of the circadian phase between the NS and DS experiments, we determined the times of nadir and peak time of cBT in both experiments. The cBT data from 18:00 h on day 2 to 24:00 h on day 3 was smoothed by using a 24-h double cosine curve fit procedure (Kaleida Graph ver.3.6, Hulinks Inc., Tokyo, Japan) for both the NS and DS experiments, and the times of the fitted minimum (nadir) and maximum (peak time) of cBTs were determined.

2.6. Statistical analyses

Differences in variables between the NS and DS experiments were analyzed by *t*-test. Differences in TEA variables for each AT between the NS and DS experiments were analyzed by two-way repeated measures ANOVA (ATs × NS vs. DS) or two-way factorial ANOVA (sleep stages just before ATs × NS vs. DS). Correlations

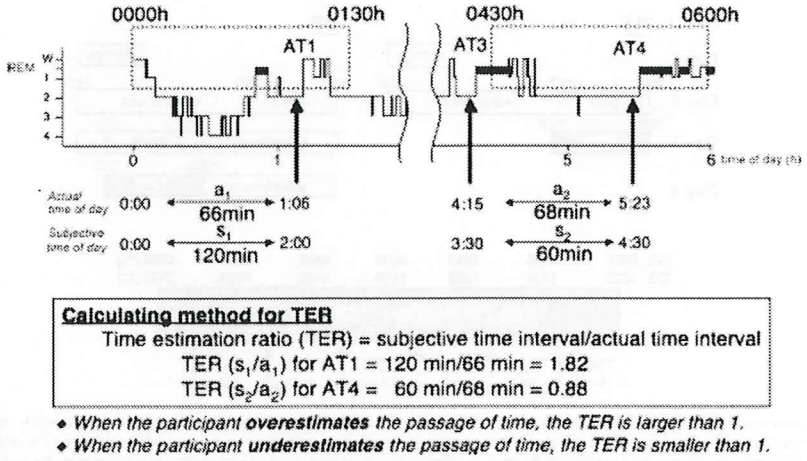

Fig. 2. Time estimation ratio (TER). Subjective time interval in both experiments was defined as the time difference between subjective times of the day, which were obtained at successive awakening trials (ATs). The actual time interval was defined as the actual time difference between successive ATs. The TER, as an indicator of subjective time estimation, was calculated by the dividing a subjective time interval (s_1 or s_2) by the actual time interval (a_1 or a_2).

Table 1
Sleep and core body temperature parameters in normal NS and DS.

	NS (n = 10) (mean ± S.D.)	DS (n = 7) (mean ± S.D.)	t-Test (p-value)
Total recording time (min)	484.5 ± 25.7	502.1 ± 20.0	n.s.
Total sleep time (min)	436.9 ± 46.8	348.3 ± 56.9	0.003
Sleep efficiency (%)	90.5 ± 10.6	69.6 ± 12.9	0.002
Wake (min)	47.5 ± 55.9	153.8 ± 68.1	0.003
Stage 1 (min)	40.2 ± 19.0	48.8 ± 19.6	n.s.
Stage 2 (min)	240.1 ± 40.6	187.9 ± 42.1	0.021
Stage 3 + 4 (min)	58.8 ± 21.9	45.4 ± 9.5	n.s.
REM (min)	65.5 ± 31.9	59.00 ± 10.1	n.s.
Wake (%)	9.5 ± 10.6	30.4 ± 12.8	0.002
Stage 1 (%)	8.3 ± 3.9	9.8 ± 4.0	n.s.
Stage 2 (%)	49.7 ± 9.1	37.6 ± 9.3	0.017
Stage 3 + 4 (%)	12.1 ± 4.5	9.0 ± 1.7	n.s.
REM (%)	13.5 ± 6.6	11.8 ± 2.1	n.s.
Core body temperature parameters			
Nadir time (h)	5.5 ± 1.3	6.3 ± 2.3	n.s.
Peak time (h)	18.9 ± 2.9	20.36 ± 4.1	n.s.

p = probability, n.s. = not significant.

between variables were assessed by Pearson's correlation coefficient. Stepwise multiple regression analysis was used to evaluate relationship between TEA variables (dependent variables) and sleep structures or circadian phase (predictor variables). StatView ver.5.0 (SAS Institute, Cary, NC, USA) was used for all statistical analyses. Data were expressed as mean ± standard deviation. The level of significance was set at $p < 0.05$.

3. Results

3.1. PSG variables

PSG variables for the entire sleep period in the NS and DS experiments are shown in Table 1. There was no significant difference in total recording time between the two experiments. Total sleep time and sleep efficiency in the DS experiment were significantly deceased in comparison to corresponding values in the NS experiment. There were no significant differences in total duration and percentages of stage 1, stage 3 + 4, or stage REM sleep between the two experiments. However, sleep total duration and percentage of stage W sleep were significantly increased and those for stage 2 sleep were significantly decreased in the DS experiment in comparison to corresponding values in the NS experiment.

3.2. Circadian phase

There was no significant difference in the time of nadir or peak time of cBT between the NS and DS experiments (Table 1).

3.3. AT variables

PSG stages during which ATs were carried out differed between the NS and DS experiments; 91.67% and 64.29% ATs, respectively, were carried out in stage 2, 6.67% and 11.1% ATs were carried out in stage 1, and 1.67% and 44.44% ATs were carried out in stage W. However, two-way factorial ANOVA (sleep stage just before ATs × NS vs. DS) revealed that there was no significant main effect of sleep stages just before ATs on TER ($F(2, 96) = 1.615$, $p = 0.204$); neither was there a significant main effect of experimental condition ($F(1, 96) = 0.908$, $p = 0.343$) nor a significant interaction ($F(2, 96) = 0.076$, $p = 0.927$) between sleep stages just before ATs and experimental condition. Therefore, the TER data obtained in the three different PSG stages (stages 1, 2, and W) were combined in further analyses.

3.4. TER

There was no significant difference in the TER for the entire sleep period between the NS and DS experiments (NS experiment, 0.966 ± 0.717; DS experiment, 1.006 ± 0.747). Time course of the TER and the percentages of sleep stages are shown in Fig. 3. Two-way repeated measures ANOVA (ATs × NS vs. DS) revealed a significant main effect of the time course on TER ($F(5, 75) = 13.254$, $p < 0.0001$), whereas there was neither a significant main effect of experimental condition ($F(1, 75) = 0.110$, $p = 0.745$) nor a significant interaction ($F(5, 75) = 0.326$, $p = 0.896$) between time course and experimental condition. The TER value was at nearly two during AT1 and gradually decreased toward 0.5 as sleep progressed. The pattern was similar in the NS and DS experiments (Fig. 3a).

3.5. Sleep structures

Two-way repeated measures ANOVA (ATs × NS vs. DS) revealed a significant main effect of time course on stage 3 + 4 ($F(5, 75) = 12.285$, $p < 0.001$), whereas there was neither a significant main effect of experimental condition ($F(1, 75) = 2.266$, $p = 0.153$) nor a significant interaction ($F(5, 75) = 0.144$, $p = 0.981$) between time course and experimental condition (Fig. 3d). Two-way repeated measures ANOVA (ATs × NS vs. DS) also revealed a significant main effect of time course on %stage 3 + 4 ($F(5, 75) = 18.333$, $p < 0.001$), whereas there was neither a significant main effect of experimental condition ($F(1, 75) = 2.436$, $p = 0.139$) nor a significant interaction ($F(5, 75) = 0.184$, $p = 0.968$) between time course and experimental condition. The stage 3 + 4 decreased as sleep progressed in both the NS and DS experiments (Fig. 3i).

There was a significant interaction between time course and conditions in stage REM, stage W, and stage 2. Stage REM in NS increased toward morning, whereas stage REM in DS decreased toward nighttime. Stage W in NS did not change toward morning, whereas stage W in DS increased from AT5 to AT6. Stage 2 in NS did not change toward morning, whereas stage 2 in DS decreased from AT5 to AT6 (Fig. 3b, c and e). No significant effect of time course was found in stage 1 in either two conditions. We also found comparable results in corresponding percentage values for all sleep stages (Fig. 3g, h and j).

3.6. Correlation between TER and sleep structures

We averaged the TER and stage 3 + 4 sleep per AT data across all participants to reduce inter-individual variation in sleep

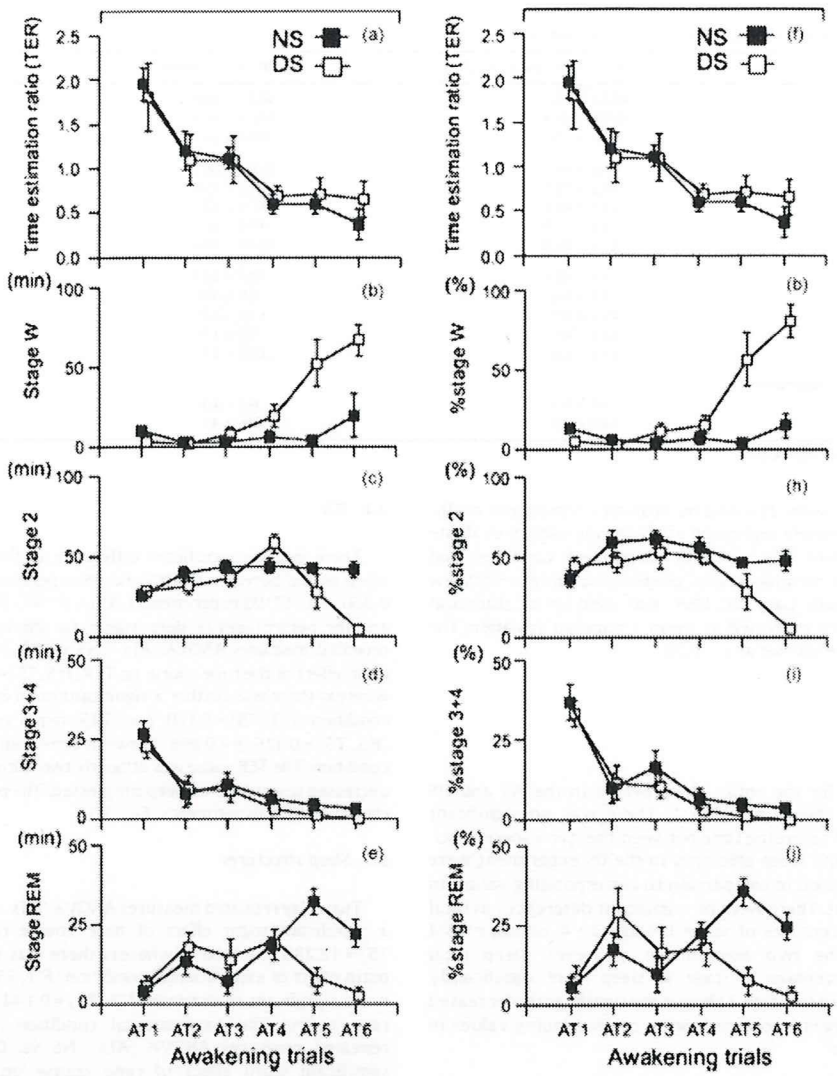

Fig. 3. (a–j) Time course of the mean time estimation ratio (TER) and the amounts (left panel) and the percentages (right panel) of sleep stages. Filled and open circles represent the data in nighttime sleep (NS) and daytime sleep (DS) experiments, respectively. The horizontal axes indicate the AT number. Two-way repeated measures ANOVA revealed a significant main effect of time course on TER and stage 3 + 4 sleep in both experiments. The value of TER was nearly 2.0 at AT1, and it decreased toward 0.5 as sleep progressed.

structure. Significant positive correlation was found between averaged TER and averaged stage 3 + 4 in both the NS ($r = 0.943$, $p = 0.002$) and DS ($r = 0.993$, $p < 0.001$). We also found a significant positive correlation between the averaged TER and averaged %stage 3 + 4 in both the NS ($r = 0.944$, $p = 0.002$) and DS ($r = 0.993$, $p < 0.001$).

3.7. Stepwise multiple regression analysis for TER

The following variables were analyzed by stepwise multiple regression for prediction of TER (dependent variable): stage W, stage 1, stage 2, stage 3 + 4, stage REM, and acrophase of each AT (interval between the time of cBT nadir and the time of each AT). Only stage 3 + 4 was identified as a predictive variable that explained the variance of TER ($r = 0.251$, $p = 0.011$). We also found comparable results in percentage values for sleep stages; only %stage 3 + 4 was identified as a more prominent predictive variable that explained the variance of TER ($r = 0.327$, $p = 0.001$).

4. Discussion

In the present study, we investigated influences of the sleep architecture on TEA during NS and DS periods. We found that TER, as an indicator of a subjectively estimated time interval, was higher at the beginning of the sleep period (i.e., sleep time was overestimated than the actual time elapsed), and that it successively decreased toward the end of the sleep. Positive correlation between the amount of SWS and the TER was confirmed in both the NS and DS periods, despite the fact that the two sleep periods were located around the circadian antiphase

represented by the cBT. This suggests that the greater the amount of SWS the study subjects obtained, the longer the sleep time they subjectively experienced. We could not confirm a steady influence of REM sleep on TEA in our study participants. We observed negative correlation between the amount of REM sleep and the TER only in the NS period, as was reported previously (Aritake et al., 2004). This relation disappeared in the DS period during which the normal REM sleep pattern was distorted (Weitzman et al., 1980; Dijk and Czeisler, 1995; Borbely and Achermann, 1999). Comparison of sleep structures and TER properties between the NS and DS periods clearly highlighted the significant influence of SWS on TEA in humans.

The study subjects experienced poorer sleep continuity (shorter total sleep time, decreased sleep efficiency, and longer awake time) in the DS period than in the NS period, possibly due to the circadian antiphase, although the amounts of stage 1, stage 3 + 4, and stage REM sleep did not differ significantly between the two experimental conditions. However, it is not likely that the differences in sleep structure during the 9-h PSG recording period substantially influenced the relation between the sleep architecture and TEA because similar TER values close to 1 were obtained (0.966 ± 0.72 for the NS period, 1.006 ± 0.75 for the DS period), suggesting that participants could accurately estimate the length of sleep time (on average) through the entire sleep period.

While the underlying regulatory mechanism of TEA during sleep remains to be clarified, various brain sites have been revealed to be responsible for human TEA of different temporal range (Ivry, 1996; Lalonde, 1999; Lewis and Miall, 2003; Ivry, 2004). For instance, the cerebellum is reported to be involved in the short time estimation of less than 1 s (Jueptner et al., 1995; Rao et al., 1997; Spencer et al., 2003; Ivry and Spencer, 2004). Contrastingly, the prefrontal cortex is involved in the time estimation of more than 1 s (Mangels et al., 1998; Lalonde and Hannequin, 1999; Lewis and Miall, 2003). Concerning the TEA during sleep, greater cortical deactivation during a longer period of SWS might contribute to overestimation of the actual sleep time. Kajimura et al. (1999) studied cerebral blood flow during sleep by means of positron emission topography. Sleep-induced cortical deactivation started during light stages of nocturnal sleep and progressed in a sleep stage-dependent manner; cerebral blood flow during deep non-REM sleep was reduced in the midbrain, basal forebrain, and basal ganglia (caudate nucleus) and bilaterally in neocortical regions including the medial and inferior frontal gyrus. During wakefulness, the cerebellum, the prefrontal cortex and basal ganglia perform higher-order processing of sensory information, integrating cognitive information. Several neuroimaging studies in humans have shown that the cerebellum, the prefrontal cortex and a corticostriatal network in the basal ganglia are responsible for the ability to perceive time intervals during wakefulness (Jueptner et al., 1995; Maquet et al., 1996; Rao et al., 1997, 2001; Harrington et al., 1998; Pouthas et al., 1999; Gruber et al., 2000; Schubotz et al., 2000; Spencer et al., 2003; Coull et al., 2004). These neuronal systems might also contribute to the regulation of TEA during sleep. Thus, preceding deep sleep and associated cortical deactivation could substantially influence perceived passage of time during sleep.

During wakefulness, TEA has been reported to show diurnal fluctuation (Aschoff, 1998; Campbell et al., 2001; Kuriyama et al., 2005). A study involving a time production strategy (producing a predetermined time interval by pressing a button) during wake time has shown that TEA might be influenced by the circadian system in humans (Kuriyama et al., 2005). The produced time interval tended to be shorter than the actual time interval during the night time, and it became longer toward the morning time. This is analogous to individuals overestimating the perceived time interval in the first half of rather than the latter half of the sleep period, as was observed in our present study. However, in our study subjects, changes in TER for the NS and DS periods in reciprocally circadian antiphase showed remarkably similar time profiles and multiple stepwise regression analysis revealed no relation between acrophases of time estimation and the corresponding TER values. Although we examined the change in TEA for only 8–9 h of each sleep periods, our findings do not support the notion that the TEA during sleep time was primarily under the regulation of circadian system.

These findings were obtained using a time estimation protocol consisted of six 90-min period interval trials, which might interfere in the naturalistic sleep cycle including REM–NREM sleep cycles and TEA properties in the study subjects. Despite of the limitations, the present study support the notion that humans possess the TEA that pervades sleep period and that SWS can prolong the subjectively estimated time interval during sleep, irrespective of the circadian phase they slept. Future studies should focus on the physiological mechanism of TEA during sleep and reveal the pathophysiological features of TEA in several sleep disorders such as paradoxical insomnia in which subjective sleep disturbances appear without objective evidence of deteriorated sleep quality (Salin-Pascual et al., 1992; Edinger and Fins, 1995; Perlis et al., 1997; Vanable et al., 2000; ICSD, 2005; Edinger and Krystal, 2003). Time estimation protocol we applied in this study would be an useful option in the human sleep studies.

Acknowledgements

This study was supported in part by a Research Grant for Nervous and Mental Disorders (11-3) and a Health Science Grant (15130301) from the Ministry of Health, Labor and Welfare of Japan, and a Grant-in-aid for Scientific Research (13470200) from the Ministry of Education, Science and Culture of Japan.

References

Aritake, S., Uchiyama, M., Tagaya, H., Suzuki, H., Kamiyama, K., Ozaki, A., Tan, X., Shibui, K., Kamei, Y., Okubo, Y., Takahashi, K., 2004. Time estimation during nocturnal sleep in human subjects. Neurosci. Res. 49, 387–393.
Aschoff, J., 1998. Human perception of short and long time intervals: its correlation with body temperature and the duration of wake time. J. Biol. Rhythms 13, 437–442.
Bell, C.R., 1972. Accurate performance of a time-estimation task in relation to sex, age, and personality variables. Percept. Mot. Skills 35, 175–178.
Borbely, A.A., Achermann, P., 1999. Sleep homeostasis and models of sleep regulation. J. Biol. Rhythms 14, 557–568.
Born, J., Hansen, K., Marshall, L., Molle, M., Fehm, H.L., 1999. Timing the end of nocturnal sleep. Nature 397, 29–30.
Campbell, S.S., 1986. Estimation of empty time. Hum. Neurobiol. 5, 205–207.
Campbell, S.S., Murphy, P.J., Boothroyd, C.E., 2001. Long-term time estimation is influenced by circadian phase. Physiol. Behav. 72, 589–593.
Coull, J.T., Vidal, F., Nazarian, B., Macar, F., 2004. Functional anatomy of the attentional modulation of time estimation. Science 303, 1506–1508.
Dijk, D.J., Czeisler, C.A., 1995. Contribution of the circadian pacemaker and the sleep homeostat to sleep propensity, sleep structure, electroencephalographic slow waves, and sleep spindle activity in humans. J. Neurosci. 15, 3526–3538.
Edinger, J.D., Fins, A.I., 1995. The distribution and clinical significance of sleep time misperceptions among insomniacs. Sleep 18, 232–239.
Edinger, J.D., Krystal, A.D., 2003. Subtyping primary insomnia: is sleep state misperception a distinct clinical entity? Sleep Med. Rev. 7, 203–214.
Fichten, C.S., Creti, L., Amsel, R., Bailes, S., Libman, E., 2005. Time estimation in good and poor sleepers. J. Behav. Med. 28, 537–553.
Gruber, O., Kleinschmidt, A., Binkofski, F., Steinmetz, H., von Cramon, D.Y., 2000. Cerebral correlates of working memory for temporal information. Neuroreport 11, 1689–1693.
Harrington, D.L., Haaland, K.Y., Knight, R.T., 1998. Cortical networks underlying mechanisms of time perception. J. Neurosci. 18, 1085–1095.
Hartocollis, P., 1980. Time and the dream. J. Am. Psychoanal. Assoc. 28, 861–877.
Hawkins, J., 1989. Sleep disturbance in intentional self-awakenings: behavior-genetic and transient factors. Percept. Mot. Skills 69, 507–510.
ICSD, 2005. ICSD-2-International Classification of Sleep Disorders, 2nd ed.: Diagnostic and Coding Manual. American Academy of Sleep Medicine.
Ivry, R.B., 1996. The representation of temporal information in perception and motor control. Curr. Opin. Neurobiol. 6, 851–857.
Ivry, R.B., Spencer, R.M., 2004. The neural representation of time. Curr. Opin. Neurobiol. 14, 225–232.

Jueptner, M., Rijntjes, M., Weiller, C., Faiss, J.H., Timmann, D., Mueller, S.P., Diener, H.C., 1995. Localization of a cerebellar timing process using PET. Neurology 45, 1540–1545.
Kaida, K., Nakano, E., Nittono, H., Hayashi, M., Hori, T., 2003. The effects of self-awakening on heart rate activity in a short afternoon nap. Clin. Neurophysiol. 114, 1896–1901.
Kajimura, N., Uchiyama, M., Takayama, Y., Uchida, S., Uema, T., Kato, M., Sekimoto, M., Watanabe, T., Nakajima, T., Horikoshi, S., Ogawa, K., Nishikawa, M., Hiroki, M., Kudo, Y., Matsuda, H., Okawa, M., Takahashi, K., 1999. Activity of midbrain reticular formation and neocortex during the progression of human non-rapid eye movement sleep. J. Neurosci. 19, 10065–10073.
Kleitman, N., 1963. Sleep and Wakefulness. Univ. Chicago Press, Chicago, pp. 122–126.
Kuriyama, K., Uchiyama, M., Suzuki, H., Tagaya, H., Ozaki, A., Aritake, S., Shibui, K., Xin, T., Lan, L., Kamei, Y., Takahashi, K., 2005. Diurnal fluctuation of time perception under 30-h sustained wakefulness. Neurosci. Res. 53, 123–128.
Lalonde, R., Hannequin, D., 1999. The neurobiological basis of time estimation and temporal order. Rev. Neurosci. 10, 151–173.
Lavie, P., Oksenberg, A., Zomer, J., 1979. It's time, you must wake up now. Percept. Mot. Skills 49, 447–450.
Lewis, P.A., Miall, R.C., 2003. Distinct systems for automatic and cognitively controlled time measurement: evidence from neuroimaging. Curr. Opin. Neurobiol. 13, 250–255.
Lewis, S.A., 1969. Subjective estimates of sleep: an EEG evaluation. Br. J. Psychol. 60, 203–208.
Mangels, J.A., Ivry, R.B., Shimizu, N., 1998. Dissociable contributions of the prefrontal and neocerebellar cortex to time perception. Brain Res. Cogn. Brain Res. 7, 15–39.
Maquet, P., Lejeune, H., Pouthas, V., Bonnet, M., Casini, L., Macar, F., Timsit-Berthier, M., Vidal, F., Ferrara, A., Degueldre, C., Quaglia, L., Delfiore, G., Luxen, A., Woods, R., Mazziotta, J.C., Comar, D., 1996. Brain activation induced by estimation of duration: a PET study. Neuroimage 3, 119–126.
Moiseeva, N.I., 1975. The characteristics of EEG activity and the subjective estimation of time during dreams of different structure. Electroencephalogr. Clin. Neurophysiol. 38, 569–577.
Moorcroft, W.H., Kayser, K.H., Griggs, A.J., 1997. Subjective and objective confirmation of the ability to self-awaken at a self-predetermined time without using external means. Sleep 20, 40–45.
Morell, V., 1996. Setting a biological stopwatch. Science 271, 905–906.
Perlis, M.L., Giles, D.E., Mendelson, W.B., Bootzin, R.R., Wyatt, J.K., 1997. Psychophysiological insomnia: the behavioural model and a neurocognitive perspective. J. Sleep Res. 6, 179–188.
Pouthas, V., Maquet, P., Garnero, L., Fernandez, A.M., Renault, B., 1999. Neural bases of time estimation: a PET and ERP study. Electroencephalogr. Clin. Neurophysiol. Suppl. 50, 598–603.
Rao, S.M., Harrington, D.L., Haaland, K.Y., Bobholz, J.A., Cox, R.W., Binder, J.R., 1997. Distributed neural systems underlying the timing of movements. J. Neurosci. 17, 5528–5535.
Rao, S.M., Mayer, A.R., Harrington, D.L., 2001. The evolution of brain activation during temporal processing. Nat. Neurosci. 4, 317–323.
Rechtschaffen, A., Kales, A., 1968. A manual of standardized terminology, techniques and scoring system for sleep stages of human subjects. Public Health Service, US Government, Printing Office, Washington DC.
Salin-Pascual, R.J., Roehrs, T.A., Merlotti, L.A., Zorick, F., Roth, T., 1992. Long-term study of the sleep of insomnia patients with sleep state misperception and other insomnia patients. Am. J. Psychiatry 149, 904–908.
Schubotz, R.I., Friederici, A.D., von Cramon, D.Y., 2000. Time perception and motor timing: a common cortical and subcortical basis revealed by fMRI. Neuroimage 11, 1–12.
Spencer, R.M., Zelaznik, H.N., Diedrichsen, J., Ivry, R.B., 2003. Disrupted timing of discontinuous but not continuous movements by cerebellar lesions. Science 300, 1437–1439.
Tart, C.T., 1970. Waking from sleep at a preselected time. J. Am. Soc. Psychosom. Dent. Med. 17, 3–16.
Vanable, P.A., Aikens, J.E., Tadimeti, L., Caruana-Montaldo, B., Mendelson, W.B., 2000. Sleep latency and duration estimates among sleep disorder patients: variability as a function of sleep disorder diagnosis, sleep history, and psychological characteristics. Sleep 23, 71–79.
Weitzman, E.D., Czeisler, C.A., Zimmerman, J.C., Ronda, J.M., 1980. Timing of REM and stages 3 + 4 sleep during temporal isolation in man. Sleep 2, 391–407.
Zepelin, H., 1986. REM sleep and the timing of self-awakenings. Bull. Psychom. Soc. 24, 254–256.
Zung, W.W., Wilson, W.P., 1971. Time estimation during sleep. Biol. Psychiatry 3, 159–164.

Sleep and Biological Rhythms 2009; 7: 17–22 doi:10.1111/j.1479-8425.2008.00377.x

ORIGINAL ARTICLE

Newly developed waist actigraphy and its sleep/wake scoring algorithm

Minori ENOMOTO,[1,2] Takuro ENDO,[3,4] Kazue SUENAGA,[4] Naoki MIURA,[5] Yasushi NAKANO,[6] Sayaka KOHTOH,[6] Yujiro TAGUCHI,[6] Sayaka ARITAKE,[1] Shigekazu HIGUCHI,[1] Masato MATSUURA,[2] Kiyohisa TAKAHASHI[7] and Kazuo MISHIMA[1]

[1]Department of Psychophysiology, National Institute of Mental Health, National Center for Neurology and Psychiatry, Tokyo, [2]Department of Life Sciences and Bio-informatics, Graduate School of Allied Health Sciences, Tokyo Medical and Dental University, Tokyo, [3]Sleep Clinic Chofu, Tokyo, [4]Aoki Hospital, Clinical Laboratory, Tokyo, [5]Central Research Insitute of Electric Power Industry, Materials Science Research Laboratory, Tokyo, [6]Kissei Comtec Co. Ltd., Nagano, [7]Aino University, Osaka, Japan

Abstract

The purpose of this study was to formulate an algorithm for assessing sleep/waking from activity intensities measured with a waist-worn actigraphy, the Lifecorder PLUS (LC; Suzuken Co. Ltd., Nagoya, Japan), and to test the validity of the algorithm. The study consisted of 31 healthy subjects (M/F = 20/11, mean age 31.7 years) who underwent one night of simultaneous measurement of activity intensity by LC and polysomnography (PSG). A sleep(S)/wake(W) scoring algorithm based on a linear model was determined through discriminant analysis of activity intensities measured by LC over a total of 235 h and 56 min and the corresponding PSG-based S/W data. The formulated S/W scoring algorithm was then used to score S/W during the monitoring epochs (2 min each, 7078 epochs in total) for each subject. The mean agreement rate with the corresponding PSG-based S/W data was 86.9%, with a mean sensitivity (sleep detection) of 89.4% and mean specificity (wakefulness detection) of 58.2%. The agreement rates for the individual stages of sleep were 60.6% for Stage 1, 89.3% for Stage 2, 99.2% for Stage 3 + 4, and 90.1% for Stage REM. These results demonstrate that sleep/wake activity in young to middle-aged healthy subjects can be assessed with a reliability comparable to that of conventional actigraphy through LC waist actigraphy and the optimal S/W scoring algorithm.

Key words: actigraphy, polysomnography, sleep/wake scoring algorithm, sleep-waking, waist-worn.

INTRODUCTION

An actigraphy is a small lightweight device for non-invasive and continuous monitoring of human rest/activity (sleep/wake) cycles.[1,2] The most commonly used actigraphy in current sleep research is a unit that is worn on the non-dominant wrist like a wristwatch for continuous measurement of forearm motor activity. The actigraphy unit generally consists of a piezoelectric accelerometer and a memory for storing the measured values for a specific time epoch, typically from 1 s to several minutes.

Algorithms using the activity level measured by the actigraphy to determine whether the person wearing the unit is awake or asleep during the time epoch have been developed for use with individual actigraphy units.[3–5] Studies to date investigating the agreement rate of polysomnography (PSG) and various actigraphy units in

Correspondence: Dr Kazuo Mishima, Department of Psychophysiology, National Institute of Mental Health, National Center of Neurology and Psychiatry, 4-1-1 Ogawa-Higashi, Kodaira, Tokyo 187-8553, Japan. E-mail: mishima@ncnp.go.jp

Accepted for publication 9 November 2008.
Published online 18 January 2009.

healthy adults have reported a very high agreement rate of 85 to 96% between the two methods with use of the optimal specific sleep/wake scoring algorithm.[3–7]

Although actigraphy is suitable for assessment of sleep/wake activity during a specific time epoch, it cannot be used independently for confirmation or diagnosis of sleep disturbances because, contrary to PSG, it does not allow for collection of data on electrooculogram (EOG), electromyogram (EMG), electrocardiogram (ECG), and breathing function during sleep.[7] On the other hand, it has a distinct advantage over PSG in that it allows for continuous recording of rest/activity (sleep/wake state) over long periods of time outside of the sleep lab with minimal disruption to the subject's normal life. It is therefore commonly used in human sleep physiology research and clinical studies in patients with insomnia and circadian rhythm sleep disorders.[6] Future beneficial applications of actigraphy include sleep disturbance screening in a large number of subjects and evaluation of the effectiveness and side effects of drug and non-drug therapies requiring continuous assessment of sleep/wake activity. Inexpensive multipurpose devices providing a favorable cost–benefit balance in the clinical setting are, however, necessary to realize these new potential applications. There have been a few previous studies that assessed sleep/wake activity using an actigraphy placed on the trunk[8,9] and the head[10] because the current mainstream wrist-worn actigraphy unit cannot be readily used in individuals with upper dystaxia, individuals with involuntary movement such as finger tremors, and children and dementia patients who may inadvertently interfere with the device. Most are also not waterproof and cannot thus readily be used in individuals whose work involves handling of water. So actigraphy units that can be worn on body sites other than the wrist, such as the trunk, are still needed.

We therefore focused our research on an inexpensive activity monitor that is worn around the waist to measure activity as a new actigraphy option in sleep research and sleep medicine. In our study, data obtained from healthy adults was used to formulate an algorithm to score sleep/waking measured by waist actigraphy and test the validity of the algorithm.

METHODS

Features of waist actigraphy

An inexpensive activity monitor that is worn around the waist (Lifecorder PLUS [LC], Suzuken Co. Ltd., Nagoya, Japan; ¥14800 = €100 = $128) was used to measure activity level during sleep. The LC was originally developed for measurement of daytime physical-activity level and has been used for the assessment of physical-activity-related energy expenditure.[11,12] The LC measures acceleration along the longitudinal axis every 4 s with an internal piezoelectric accelerometer and classifies the intensity into 11 levels from 0 to 9 (0, 0.5, 1, 2, 3, 4, 5, 6, 7, 8, 9) every 2 min.[11] Level 0 (corresponding to <0.06 G) denotes immobility and Levels 0.5 to 9 (corresponding to ≥0.06 G) denote subtle to strong movements. The cut-off point of activity intensity (the acceleration value) for each level is not provided by the manufacturer. It is possible to continuously record the activity intensity level with the time information for at least 2 months. After the completion of measurement, the recorded activity intensity data can be downloaded to a personal computer through a USB cable. The scoring algorithm was formulated from these data.

Experimental subjects

The study consisted of 31 healthy adults (20 males and 11 females with a mean age of 31.6 ± 10.4 years). Monitoring was performed by the Sleep Electroencephalography Lab at Aoki Hospital and the Sleep/Biological Rhythm Monitoring Unit of the National Institute of Mental Health of the National Center of Neurology and Psychiatry. Subjects underwent simultaneous continuous monitoring of intensity of physical movement during sleep by PSG and LC. The study was approved by the ethics committee of the National Center of Neurology and Psychiatry. Subjects were informed of the purposes and methods of the study and gave written consent to participate in the investigation.

PSG and LC recordings

The PSG consisted of measurement of a standard electroencephalogram (C3-A2, C4-A1, O1-A2, O2-A1), EOG, chin EMG, ECG, breathing function, and tibialis anterior EMG data every 30 s. The Polymate 1524 (TEAC Corporation, Tokyo, Japan) and Comet PSG (Grass-Technologies, RI, USA) were used for the PSG. The sleep stage (Stage 1, Stage 2, Stage 3 + 4, Stage REM or Stage wake) was then determined every 30 s according to the rules of Rechtschaffen and Kales.[13] Four consecutive 30-s intervals of sleep stage data were used to assess sleep/wake state every 2 min to correspond with the intervals with LC data. When four consecutive data contained two or more of Stage wake, the data set was classified as wake (W_{PSG}) according to the definition

adopted the previous studies.[14–16] All other data sets were classified as sleep (S_{PSG}). Furthermore, S_{PSG} was subclassified as Stage REM, Stage 1, Stage 2, or Stage 3 + 4, according to the most frequent sleep stage in the data set (e.g. when S_{PSG} contained two or more Stage 1 data, it was classified as Stage 1). However, when S_{PSG} contained two of two different stages, the priority order (Stage REM → Stage 1 → Stage 2 → Stage 3 + 4) was used (e.g. when S_{PSG} contained two Stage 1 and two Stage REM, it was classified as Stage REM).

Formulation of an algorithm for assessing sleep/waking

A S/W scoring algorithm for LC was newly formulated by the discriminant analysis. The data used for the development were the datasets of S_{PSG} (=0) and W_{PSG} (=1) corresponding to the LC exercise intensities obtained from 7078 epochs obtained from 31 subjects on 31 nights over a total of 235 h and 56 min.

Taking the S/W algorithm for the present actigraphy into account, we assume the five-dimension linear model that incorporates the exercise intensities during 10 min with the center of the time epoch of interest. The activity intensities 4 min before the scored epoch, 2 min before the scored epoch, during the scored epoch, 2 min after the scored epoch, and 4 min after the scored epoch were represented by x_1, x_2, x_3, x_4, and x_5, respectively. A linear discriminant function was given as the following equation for an arbitrary set of weight coefficients of a_1, a_2, a_3, a_4, and a_5.

$$z = a_1x_1 + a_2x_2 + a_3x_3 + a_4x_4 + a_5x_5$$

Where the variable of z can be used as the discriminant score to classify a set of activity intensities into the stage of S_{LC} or W_{LC}.

The above discriminant function was determined by the discriminant analysis. Supposing that the LC activity intensity in sleeping status and in waking status are categorized in class 1 and 2, respectively, and the number of the datasets in each class is set to n_1 and n_2, the i-th ($i = 1$ to n_k) variable in class k ($k = 1, 2$), $z_i^{(k)}$ is given as

$$z_i^{(k)} = a_1x_{1i}^{(k)} + a_2x_{2i}^{(k)} + a_3x_{3i}^{(k)} + a_4x_{4i}^{(k)} + a_5x_{5i}^{(k)}.$$

The variation of $\{z_i^{(k)}\}$ is represented by the total sum of squares, S_T, which can be decomposed to the between sum of squares, S_B, and the within sum of the squares, S_W ($S_T = S_B + S_W$).

$$S_T = \sum_{k=1}^{2}\sum_{i=1}^{n_k}(z_i^{(k)} - \bar{z})^2$$

$$S_B = \sum_{k=1}^{2} n_k(\bar{z}^{(k)} - \bar{z})^2$$

$$S_W = \sum_{k=1}^{2}\sum_{i=1}^{n_k}(z_i^{(k)} - \bar{z}^{(k)})^2.$$

Since the better discriminability between the two classes using z is equivalent to the increase of the ratio of correlation, $\eta^2 = S_B / S_T$, the set of weight coefficients, $\hat{a}_1$, $\hat{a}_2$, $\hat{a}_3$, $\hat{a}_4$, $\hat{a}_5$, that gives the maximum η^2 can be calculated by the following equations:

$$\begin{bmatrix} s_{11} & s_{12} & s_{13} & s_{14} & s_{15} \\ s_{21} & s_{22} & s_{23} & s_{24} & s_{25} \\ s_{31} & s_{32} & s_{33} & s_{34} & s_{35} \\ s_{41} & s_{42} & s_{43} & s_{44} & s_{45} \\ s_{51} & s_{52} & s_{53} & s_{54} & s_{55} \end{bmatrix} \begin{bmatrix} \hat{a}_1 \\ \hat{a}_2 \\ \hat{a}_3 \\ \hat{a}_4 \\ \hat{a}_5 \end{bmatrix} = \begin{bmatrix} \bar{x}_1^{(1)} - \bar{x}_1^{(2)} \\ \bar{x}_2^{(1)} - \bar{x}_2^{(2)} \\ \bar{x}_3^{(1)} - \bar{x}_3^{(2)} \\ \bar{x}_4^{(1)} - \bar{x}_4^{(2)} \\ \bar{x}_5^{(1)} - \bar{x}_5^{(2)} \end{bmatrix}.$$

Where $\bar{x}_j^{(k)}$ is the average of the j-th variable in class k, $s_{jj'}$ is the within covariance between the j-th and j'-th variables. They are evaluated by

$$\bar{x}_j^{(k)} = \frac{1}{n_k}\sum_{i=1}^{n_k} x_{ji}^{(k)}$$

$$s_{jj'} = \frac{1}{n_1 + n_2 - 2}\sum_{k=1}^{2}\sum_{i=1}^{n_k}(x_{ji}^{(k)} - \bar{x}_j^{(k)})(x_{j'i}^{(k)} - \bar{x}_{j'}^{(k)}).$$

S/W agreement rate

The S/W scoring algorithm was used to determine the S_{LC}/W_{LC} state from the activity intensity data in a total of 7078 epochs in the 31 subjects, and the agreement rate with the corresponding S_{PSG}/W_{PSG} results was calculated by subject and sleep stage. The agreement rate with the PSG-based sleep epochs (sensitivity) and agreement rate with the PSG-based wakefulness epochs (specificity) were also calculated by subject. SPSS version 11.5 was used for the statistical analysis (SPSS Japan Inc., Tokyo, Japan). Results were expressed as mean ± SD.

RESULTS

S/W scoring algorithm

The following S/W scoring algorithm was derived from the results of discriminant analysis of the activity

Table 1 Sleep parameters scored by polysomnography (PSG) and Lifecorder (LC) data

Sleep parameters	PSG	LC	Significance
Sleep efficiency (%)	90.2 ± 9.6 (61.8–99.1)	86.8 ± 11.1 (44.1–100.0)	$t(60) = 1.26$, $P = 0.21$
Total sleep time (min)	406.6 ± 78.9 (179.3–587.0)	376.3 ± 76.3 (208.0–586.0)	$t(60) = 1.53$, $P = 0.13$
Wake after sleep onset (min)	45.2 ± 48.3 (3.67–232.7)	59.9 ± 68.5 (0–388.0)	$t(60) = 0.98$, $P = 0.33$

Table 2 Decision parameters of S/W prediction algorithm for the Lifecorder

			Number of epochs
Agreement rates (%)	Overall	86.9 ± 8.9	7078
	Stage W	58.2 ± 30.4	819
	Stage 1	60.6 ± 26.2	427
	Stage 2	89.3 ± 10.6	3604
	Stage 3 + 4	99.2 ± 2.1	838
	Stage REM	90.1 ± 17.5	1300
Sensitivity (%)		89.4 ± 10.6	
Specificity (%)		58.2 ± 30.4	
Percentage of S_{PSG} epochs misscored as W_{LC} (%)		10.6 ± 10.6	
Percentage of W_{PSG} epochs misscored as S_{LC} (%)		41.8 ± 30.4	

S, sleep; W, wakefulness.

intensity data and PSG-based sleep/wake data from the total 7078 epochs obtained from 31 subjects:

$$z = 0.635x_1 + 0.427x_2 + 0.701x_3 + 0.805x_4 + 0.718x_5$$

where $z \geq 1$ indicates wakefulness (W_{LC}) and $z < 1$ indicates sleep (S_{LC}).

The linear discriminant function was transformed in advance by using linearity of the discriminant function in such a way that the threshold (z) becomes 1. Here, x_1, x_2, x_3, x_4, and x_5 indicate the activity intensity 4 min before the scored epoch, 2 min before the scored epoch, during the scored epoch, 2 min after the scored epoch, and 4 min after the scored epoch.

Validity of the S/W scoring algorithm

The sleep parameters derived from PSG and the LC activity intensity data are shown in Table 1. Sleep efficiency, total sleep time, and wakefulness after sleep onset were each derived from PSG and the LC activity intensity data (Table 1). No statistically significant differences were observed between PSG and the LC in any of the sleep parameters.

Table 2 shows the sleep/wake agreement rates between the LC and PSG, and the sensitivity and specificity of the LC. The overall agreement rate between the LC and PSG in the 31 subjects was 86.9 ± 8.9%. By sleep stage, the Stage 1 agreement rate was low at approximately 60%, but the Stage 2, Stage REM, and Stage 3 + 4 agreement rates were high at approximately 90% for Stage 2 and Stage REM and close to 100% for Stage 3 + 4.

The S/W scoring algorithm had a mean sensitivity (S detection) of 89.4 ± 10.6% and a mean specificity (W detection) of 58.2 ± 30.4%. In other words, 10.6 ± 10.6% of S_{PSG} were misscored as W_{LC} and 41.8 ± 30.4% of W_{PSG} were misscored as S_{LC}.

Activity intensity distribution before and after the scored epoch

Figure 1 shows the mean activity intensity recorded by the LC for nine consecutive epochs (18 min) centered at the W_{PSG} epoch (averaged for a total of W_{PSG} 819 epochs obtained from 31 subjects). The mean activity intensity recorded by the LC peaked just after the W_{PSG} epoch.

DISCUSSION

In the study, an S/W scoring algorithm for the LC was formulated through linear-based discriminant analysis of the corresponding longitudinal "PSG-based sleep/wake state" and "LC-recorded activity intensity" data in 7078 epoch recordings in 31 subjects over a total of

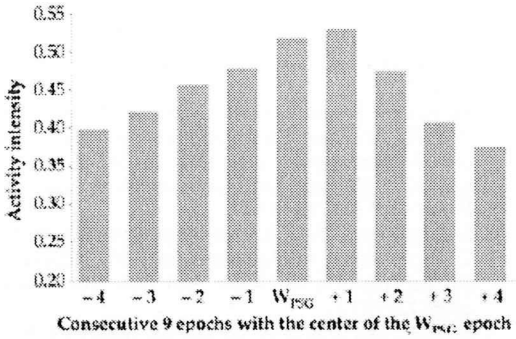

Figure 1 Activity intensity distribution before and after the scored epoch. The mean activity intensity recorded by the Lifecorder (LC) for nine consecutive epochs (18 min) centered at the W_{PSG} epoch. Vertical bars indicate the activity intensity. The mean activity intensity bars formed an inverted U-shape and peaked just after the W_{PSG} epoch.

2.35 h and 56 min. Comparison of the S/W activity determined from the LC data through the S/W scoring algorithm and the comparable activity determined from the PSG data through the rules of Rechtschaffen and Kales showed a mean agreement rate of approximately 87% in the 31 subjects. This rate is comparable to the 85 to 96% agreement rates obtained with conventional actigraphy units and their S/W scoring algorithms.[3–7] The LC and its S/W scoring algorithm yielded a high agreement rate of 90% or greater for Stage 2 and Stage 3 + 4 deep sleep and REM sleep, as well as an approximately 60% agreement rate for W_{PSG}, which is higher than that yielded by conventional algorithms. In order to examine the superiority of the five-dimensional model over the three-, seven-, or nine-dimensional models, we assumed linear models which incorporate the activity intensities during intervals of 6, 14, and 18 min centered at the time epoch of interest. The total agreement rates of the algorithms for the three-, five-seven-, and nine-dimensional models were 82.9%, 86.9% 86.0%, and 87.3%, respectively. Finally, we adopted the algorithm of the five-dimensional model since the agreement rate appeared to become saturated for models with more than five-dimensions. These findings show that when used with the S/W scoring algorithm developed in the study, the LC is a useful sleep assessment device with equivalent S/W identification capacity to conventional actigraphy systems.

Silent awakeness has been generally difficult to detect through actigraphic S/W assessment, in which it may be misscored as sleep, resulting in a pattern of overassessment of total sleep time and sleep efficiency compared to PSG-based assessment.[4,16,17] The LC and the S/W scoring algorithm derived in this study did not, however, result in a pattern of over-identification of S_{LC}, but contrarily yielded lower total sleep time and sleep efficiency values than the S_{PSG}/W_{PSG} assessment (Table 1). The specificity of the S/W scoring algorithm for the LC (58.2%) is in fact higher than that for conventional actigraphy units and their S/W scoring algorithms (40.6 vs 44%),[4,17] demonstrating that the S/W scoring algorithm for the LC developed in the study allows for more accurate identification of W_{LC}.

The S/W detection algorithm for wrist actigraphy used in a previous study assigned the highest weighting coefficient to the scored epoch.[4] However, in the S/W scoring algorithm for the LC, the highest weighting coefficient was assigned to the period immediately following the scored epoch. In fact, the mean activity intensity recorded by the LC peaked just after the W_{PSG} epoch (Fig. 1), and the delayed increase in truncal movement after awakening characterized the highest weighting coefficient assigned immediately after the scored epoch.

The LC is worn on the trunk while the conventional actigraphies used to be worn on the non-dominant wrist.[3–7] This may be related to the high specificity of the LC and its S/W scoring algorithm. The different application sites mean that S/W activity is assessed through different types of movement during sleep, either extremity or trunk movement (which are often independent),[18,19] which may produce the differences in assessment noted above. The LC and its S/W scoring algorithm investigated in the current study may more accurately detect silent awakeness due to the sensitivity to small movements of the torso during sleep and a resulting higher composite variable z value.

There are several issues that require further exploration with respect to use of the LC as a novel option for sleep assessment. First, the time epoch of S/W scoring algorithms for conventional actigraphy is often 1 min or less.[3,5,14] The time epoch for the LC used in this study is 2 min, leading to the assumption that devices with higher temporal resolution may result in higher agreement rates. Although it is more expensive (¥37 000 = €230 = $350), there is an LC that is programmable to 4-s time epochs. It would therefore be of merit to formulate an S/W scoring algorithm for this LC to determine whether it yields a higher agreement rate. Second, the S/W scoring algorithm formulated in the study uses the data from the scored time epoch as well as the data from the two epochs (4-min interval) immediately prior

and immediately after to scoring S/W. This means that activity intensity data prior to onset of sleep will be included in the scoring formula for the scored time epoch unless at least 4 min have passed from the onset of sleep on PSG. This complicates detection of differences in sleep latency of the order of several minutes. Accordingly, sleep latency was not analyzed in this study. This perhaps poses a constraint to the use of the I.C in studies and tests requiring accurate evaluation of sleep latency. It is expected that development of I.Cs with higher temporal resolution and their S/W scoring algorithms will solve this issue.

In the current study, an S/W scoring algorithm for the I.C was formulated from the data of young to middle-aged healthy adults and the validity of the algorithm was tested. Other potential useful applications of the inexpensive I.C include sleep disorder screening in a large number of individuals. In the future, it will be necessary to determine whether the high agreement rates can also be obtained when the I.C and its S/W scoring algorithm are used to assess sleep/wake activity in subjects from different age groups, including children and the elderly, and in patients with common sleep disorders, such as insomnia and sleep respiratory disturbances.

ACKNOWLEDGMENTS

This study was supported by a Grant-in-Aid for Cooperative Research from the Ministry of Health, Labor, and Welfare of Japan (H19-kokoro-ippan-013, H20-tyojyu-ippan-001).

There was no additional private funding for the study, either from Suzuken Co. Ltd. or any other source. Co-authors Y.N., S.K., and Y.T. are currently developing clinical software using the sleep/wake scoring algorithm formulated in the study, but they did not contribute to the funding of the study.

REFERENCES

1 Kupfer DJ, Foster FG. Sleep and activity in a psychotic depression. *J. Nerv. Ment. Dis.* 1973; **156**: 341–8.
2 Kripke DF, Mullaney DJ, Messin S, Wyborney VG. Wrist actigraphic measures of sleep and rythms. *Electroencephalogr. Clin. Neurophysiol* 1978; **44**: 674–6.
3 Webster JB, Kripke DF, Messin S, Mullaney DJ, Wyborney G. An activity-based sleep monitor system for ambulatory use. *Sleep* 1982; **5**: 389–99.
4 Cole RJ, Kripke DF, Gruen W, Mullaney DJ, Gillin JC. Automatic sleep/wake identification from wrist activity. *Sleep* 1992; **15**: 461–9.
5 Jean-Louis G, Kripke DF, Cole RJ, Assmus JD, Langer RD. Sleep detection with an accelerometer actigraph: comparisons with polysomnography. *Physiol. Behav.* 2001; **72**: 21–8.
6 Ancoli-Israel S, Cole R, Alessi C, Chambers M, Moorcroft W, Pollak CP. The role of actigraphy in the study of sleep and circadian rhythms. *Sleep* 2003; **26**: 342–92.
7 Acebo C, Lebourgeois MK. Actigraphy. *Respir. Care Clin. N. Am.* 2006; **12**: 23–30.
8 Kochersberger G, McConnell E, Kuchibhatla MN, Pieper C. The reliability, validity, and stability of a measure of physical activity in the elderly. *Arch. Phys. Med. Rehabil.* 1996; **77**: 793–5.
9 Paavonen EJ, Fjallberg M, Steenari MR, Aronen ET. Actigraph placement and sleep estimation in children. *Sleep* 2002; **25**: 235–7.
10 Spivak E, Oksenberg A, Catz A. The feasibility of sleep assessment by actigraph in patients with tetraplegia. *Spinal Cord.* 2007; **45**: 765–70.
11 Kumahara H, Schutz Y, Ayabe M *et al.* The use of uniaxial accelerometry for the assessment of physical-activity-related energy expenditure: a validation study against whole-body indirect calorimetry. *Br. J. Nutr.* 2004; **91**: 235–43.
12 Saito N, Yamamoto T, Sugiura Y, Shimizu S, Shimizu M. Lifecorder: a new device for the long-term monitoring of motor activities for Parkinson's disease. *Intern. Med.* 2004; **43**: 685–92.
13 Rechtschaffen A. A manual of standardized terminology, technique and scoring system for sleep stages of human subjects. Los Angeles, CA: Brain Information Service/Brain Research Institute, UCLA. 1968.
14 Sadeh A, Sharkey KM, Carskadon MA. Activity-based sleep-wake identification: an empirical test of methodological issues. *Sleep* 1994; **17**: 201–7.
15 Lotjonen J, Korhonen I, Hirvonen K, Eskelinen S, Myllymaki M, Partinen M. Automatic sleep-wake and nap analysis with a new wrist worn online activity monitoring device vivago WristCare. *Sleep* 2003; **26**: 86–90.
16 Paquet J, Kawinska A, Carrier J. Wake detection capacity of actigraphy during sleep. *Sleep* 2007; **30**: 1362–9.
17 de Souza L, Benedito-Silva AA, Pires ML, Poyares D, Tufik S, Calil HM. Further validation of actigraphy for sleep studies. *Sleep* 2003; **26**: 81–5.
18 Van Hilten JJ, Middelkoop HA, Kuiper SI, Kramer CG, Roos RA. Where to record motor activity: an evaluation of commonly used sites of placement for activity monitors. *Electroencephalogr. Clin. Neurophysiol.* 1993; **89**: 359–62.
19 Middelkoop HA, van Dam EM, Smilde-van den Doel DA, Van Dijk G. 45-hour continuous quintuple-site actimetry: relations between trunk and limb movements and effects of circadian sleep-wake rhythmicity. *Psychophysiology* 1997; **34**: 199–203.

Psychiatry and Clinical Neurosciences 2009; 63: 209–217 doi:10.1111/j.1440-1819.2009.01941.x

Regular Article

Hyperfrontality in patients with schizophrenia during saccade and antisaccade tasks: A study with fMRI

Mai Fukumoto-Motoshita, MMS,[1,2] Masato Matsuura, MD, PhD,[3] Tatsunobu Ohkubo, MD, PhD,[4] Hiromi Ohkubo, MD, PhD,[4] Noriko Kanaka, BA,[1,4] Eisuke Matsushima, MD, PhD,[2] Masato Taira, DDS, PhD,[5] Takuya Kojima, MD, PhD[1,4,6] and Tetsuya Matsuda, PhD[1]*

[1]*Tamagawa University Brain Science Institute,* [2]*Section of Liaison Psychiatry & Palliative Medicine, Graduate School of Tokyo Medical & Dental University ,* [3]*Section of Biofunctional Informatics, Graduate School of Allied Health Sciences, Tokyo Medical and Dental University,* [4]*Department of Neuropsychiatry, Nihon University School of Medicine,* [5]*Advanced Research Institute for the Sciences and Humanities, Nihon University, Tokyo and* [6]*Ohmiya-Kosei Hospital, Saitama, Japan*

Aims: Antisaccadic eye movements, requiring inhibition of a saccade toward a briefly appearing peripheral target, are known to be impaired in schizophrenia. Previous neuroimaging studies have indicated that patients with schizophrenia show diminished activations in the frontal cortex and basal ganglia. These studies used target fixation as a baseline condition. However, if the levels of brain activities at baseline are not compatible between patients and healthy subjects, between-group comparison on antisaccade-related activations is consequently invalidated. One possibility is that patients with schizophrenia may present with greater activation during fixation than healthy subjects. In order to examine this possibility, here we investigated brain activities associated with antisaccade in the two groups without using target fixation at baseline.

Methods: Functional brain images were acquired during prosaccades and antisaccades in 18 healthy subjects and 18 schizophrenia patients using a boxcar functional magnetic resonance imaging design. Eye movements were measured during scanning.

Results: In the patient group, the elevated activities in the dorsolateral prefrontal cortex (DLPFC) and thalamus, normally seen in antisaccade tasks relative to saccade tasks, were no longer observed. Moreover, in normal subjects, activities in the DLPFC and thalamus were greater during the antisaccade task than during the saccade task. In patients, no such difference was observed between the two tasks, suggesting that these brain regions are likely to be highly activated even by a simple task such as fixation. In particular, the DLPFC and thalamus in patients were not activated at a level commensurate with the difficulty of the tasks presented.

Conclusions: From these results, it is suggested that schizophrenia entails dysfunctions in the fronto-striato-thalamo-cortical network associated with motor function control.

Key words: antisaccade, fMRI, hyperfrontality, saccade, schizophrenia.

SACCADIC EYE MOVEMENTS are the primary mechanism used by primates to visually explore their environments. A visually guided reflexive saccade can be defined as an automatic orienting response to a novel visual target in the peripheral field. Patients with schizophrenia perform prosaccades normally, making rapid and accurate eye movements to targets.[1–3] In contrast, the inhibition of

**Correspondence: Tetsuya Matsuda, PhD, Tamagawa University Brain Science Institute, 6-1-1, Tamagawa Gakuen, Machida, Tokyo 194-8610, Japan. Email: tetsuya@lab.tamagawa.ac.jp*

Received 18 August 2008, revised 26 November 2008; accepted 3 December 2008.

automatic saccades is impaired in schizophrenic patients.[4] One task used to investigate saccade inhibition is the antisaccade task, which requires subjects to inhibit a saccade toward a briefly appearing peripheral target, and to instead immediately generate a saccade to a point in the opposite direction.[5] Antisaccade deficits have high sensitivity and high specificity for the diagnosis of schizophrenia and are thought to be a genetic marker for the illness. Reported rates of antisaccade deficits range from 24% to 71% in patients with schizophrenia and from 2% to 27% in normal controls.[6–9]

Several comparison studies to date have examined the brain regions associated with antisaccade tasks in schizophrenic patients and normal control subjects.[10–12] Most of these have reported reduced activity in the basal ganglia and the cortex, including the prefrontal area, in the schizophrenic group. As we will discuss further below, we question whether the activities of these brain regions were in fact reduced or not. Functional magnetic resonance imaging (fMRI) is a specialized MRI scan that measures hemodynamic responses related to neural activity in the brain. When two actions that generate neural activity are compared in fMRI, an analysis is based on the difference between a baseline signal and a signal measured at the time of task execution. Therefore, when comparing two groups, it is important to be able to assume that the baseline levels in the two groups are equivalent. Most previous fMRI research on antisaccade and saccade tasks used a target that required subjects to focus on a central fixation point during baseline imaging. One possibility is that patients with schizophrenia may exhibit greater cerebral activities during the fixation condition than healthy subjects. In order to examine this baseline effect, here we compared schizophrenic patients and normal subjects using a blank screen on which subjects were not required to focus at baseline.

MATERIALS AND METHODS

Subjects

Eighteen patients with schizophrenia (11 men and 7 women; mean age 34.8 ± 7.9) and 18 healthy subjects (9 men and 9 women; mean age 37.6 ± 4.8) participated in this study. All patients met the criteria for schizophrenia according to the DSM-IV. The mean duration of education was significantly longer ($P < 0.05$) in the healthy subject group than in the schizophrenia group. In the latter group, the mean age at onset of psychosis was 25.8 years old, the mean Brief Psychiatric Rating Scale total score was 41.9, and the mean total dose of antipsychotic medication per patients converted to haloperidol equivalency was 16.0 mg. All healthy subjects were free from neurological or psychiatric illness, and no abnormalities were observed on brain structural MRI. Written informed consent was obtained from all participants. All participants were right-handed according to the Edinburgh Handedness Inventory.[13] This project was conducted in accordance with the Declaration of Helsinki and approved by the Ethical Committee of Nihon University School of Medicine.

MRI acquisition

MRI data were acquired using a 1.5T Siemens Symphony system (Siemens, Erlangen, Germany). Gradient-recalled echo planar imaging (EPI) was used for the fMRI sequence to obtain blood oxygen level-dependent contrast. Interleaved multi-slice gradient EPI was used to produce 40 continuous, 3-mm thick axial slices encompassing the entire brain (echo time = 62 ms, repetition time = 4000 ms, flip angle = 90 degrees, field of view = 192 mm, 64*64 matrix). Each series comprised 104 scans with a complete duration of 416 s. The run began with four dummy volumes to allow for T1 equilibration effects. The head of the subject was fixed using cushions to minimize motion artifacts.

Behavioral methods

Saccade and antisaccade performance was recorded outside of the magnet. Horizontal and vertical eye movements and target position were measured using electro-oculography (EOG) (NEC) and a goggles-type display (SONY).

Stimulus projection

The stimulus was generated using a personal computer (OS: Windows 98) and made to order software. The stimulus was projected on a small screen attached to a head coil, using a liquid crystal display projector system customized to our MRI machine (Kiyohara Optics, Tokyo).

Prosaccade task

Each trial began with the target in central fixation (0 degrees) for a random duration of 500–1500 ms.